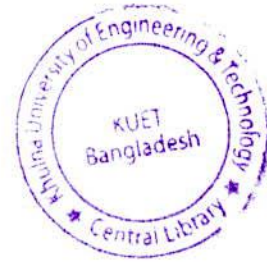i

Improvement of BER Performance of DS-OCDMA in Dispersive Fiber Medium

by

(Md. Jahedul Islam)

A thesis submitted in partial fulfillment of the requirements for the degree of
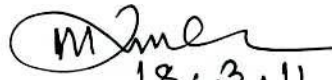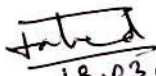Master of Science in Electrical and Electronic Engineering

Khulna University of Engineering & Technology
Khulna-9203, Bangladesh

March 2011

Declaration

This is to certify that the thesis work entitled "*Improvement of BER Performance of DS-OCDMA in Dispersive Fiber Medium*" has been carried out by *Md. Jahedul Islam* in the department of Electrical and Electronic Engineering, Khulna University of Engineering & Technology, Khulna, Bangladesh. The above thesis work or any part of this work has not been submitted anywhere for the award of any degree or diploma.
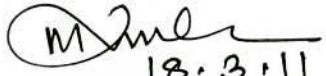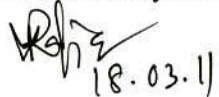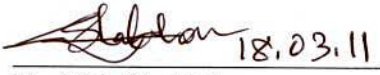
18.3.11
Signature of Supervisor

18.03.11
Signature of Candidate

Approval

This is to certify that the thesis work submitted by *Md. Jahedul Islam* entitled "*Improvement of BER Performance of DS-OCDMA in Dispersive Fiber Medium*" has been approved by the board of examiners for the partial fulfillment of the requirements for the degree of *M. Sc. Engineering* in the Department of *Electrical and Electronic Engineering*, Khulna University of Engineering & Technology, Khulna, Bangladesh in March 2011.

BOARD OF EXAMINERS

1. _____
18.3.11

Dr. Md. Rafiqul Islam
Professor
Department of Electrical and Electronic Engineering
Khulna University of Engineering & Technology

Chairman
(Supervisor)

2. _____
18.03.11

Dr. Md. Abdur Rafiq
Head of the Department
Department of Electrical and Electronic Engineering
Khulna University of Engineering & Technology

Member

3. _____
18.03.11

Dr. Md. Abdur Rafiq
Professor
Department of Electrical and Electronic Engineering
Khulna University of Engineering & Technology

Member

4. _____
18.03.11

Dr. Md. Shahjahan
Associate Professor
Department of Electrical and Electronic Engineering
Khulna University of Engineering & Technology

Member

5. _____
18/03/2011

Dr. Md. Ruhul Amin
Professor
Department of Electrical and Electronic Engineering
Rajshahi University of Engineering & Technology

Member
(External)

Acknowledgements

First of all my gratitude and thanks to almighty ALLAH for successful completion of my thesis.

I would like to use this opportunity to express my sincere gratitude to my supervisor, Dr. Md. Rafiqul Islam, Professor, Department of Electrical and Electronic Engineering, KUET, for his continuous encouragement, advice and motivation that enabled me to achieve all goals to complete this research to the best of my standard.

I am very thankful to Dr. Md. Abdur Rafiq, Professor and Head of the Department of EEE, KUET, for his support, and providing the departmental facilities for the completion of this research work.

I am also grateful to Dr. Md. Shahjahan, Associate Professor, Department of EEE, KUET, for his valuable discussion on this work.

I would like to thank Dr. Md. Ruhul Amin, Professor, Department of Electrical and Electronic Engineering, RUET, for his valuable suggestions to complete this research work.

Furthermore, I would like to thank all the faculty members of EEE department, KUET for helping in various ways in formatting this dissertation.

Finally, I expand my earnest thanks to my family members and particularly to my beloved mother.
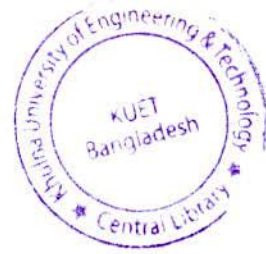
Abstract

Among the dispersion mechanisms fiber group velocity dispersion (GVD) and polarization mode dispersion (PMD) are the key limiting factors for high-speed, long length and high-performance fiber optic communications, especially, for optical code division multiple access (OCDMA). In this study, an analytical model is proposed to evaluate the bit error rate (BER) performance of direct sequence (DS) OCDMA with cascaded in-line optical amplifiers in presence of GVD, PMD, and their compensations using fiber Bragg grating (FBG) and frequency advanced higher-order PMD vectors. Optical orthogonal codes (OOC) are used as address sequence, and Intensity modulation direct detection technique is employed in a single mode fiber optic system operating at 1550nm. Optoelectronic conversion is performed by an avalanche photodiode (APD) in an optical correlator receiver. The system BER performance is determined on account of receiver, optical amplifier, and multiple access interference (MAI) noises. The power penalty suffered by the system is determined at BER of 10^{-9} as a function of system parameters.

The BER performance of the proposed OCDMA system is investigated in two steps. The impact of GVD and its compensation is studied in the first step taking into account of super Gaussian and Hyperbolic-Secant-shaped OOC's as address sequence. In the second step the influence of PMD and its compensation is analyzed under GVD-induced penalty compensated condition. The results obtained in the first step indicate that the performance of proposed system severely degrades due to interchip interference caused by GVD-induced spreading and overlapping of short duration chips which limits the fiber length, chip rate, and number of simultaneous user. The numerical results also indicate that the system BER performance is highly dependent on the chipshape, and suffers minimum penalty when Hyperbolic-Secant-shaped chip is used instead of super-Gaussian-shaped chip. The system performance is further determined in presence of FBG-based compensator. It is found that about 90% of the GVD-induced penalty can be compensated depending on the compensator parameters.

In the second step, the BER performance of proposed DS-OCDMA system is evaluated in presence of PMD and PMD compensation using Gaussian shaped OOC's. The system BER performance is found to degrade more at higher chip rate, and longer fiber length due to the effect of PMD. However, employing PMD compensation significant improvement of the system performance is found by third-order PMD compensation with respect to first-, and second-order compensations.

Contents

List of Figures

List of Abbreviations

ACF	Autocorrelation function
APD	Avalanche photodiode
BER	Bit Error Rate
CCF	Cross-correlation function
CDMA	Code Division Multiple Access
dBm	Decibel relative to 1mw
DCF	Dispersion Compensating Fiber
DGD	Differential group delay
DS	Direct sequence
DWDM	Dense WDM
EDFA	Erbium doped fiber amplifier
Erfc	Complementary error function
FBG	Fiber Bragg Grating
FH	Frequency hop
FWM	Four Wave Mixing
GF	Galois Field
GVD	Group Velocity Dispersion
IM/DD	Intensity modulation direct detection
ITU	International telecommunication union
LAN	Local area network
LASER	Light amplification by stimulated emission of radiation
LD	Laser diode
MAI	Multiple Access Interference
MAN	Metropolitan area network
MSSI	Mid-span spectral inversion
OCDMA	Optical CDMA
OGL	Optimum grating length

OOC	Optical orthogonal code
OOK	On-Off Keying
OTDMA	Optical TDMA
PDF	Probability density function
PDG	Polarization-dependent gain
PDL	Polarization-dependent loss
PLC	Planar lightwave circuit
PMD	Polarization mode dispersion
PPM	Pulse Position Modulation
PS	Prime sequence
QC	Quadratic congruence
RFI	Radio frequency interference
SDH	Synchronous digital hierarchy
SNR	Signal to Noise Ratio
SOP	State of polarization
SOPMD	Second-order PMD
SPM	Self Phase Modulation
SS	Spread spectrum
TDMA	Time Division Multiple Access
VAD	Vapour axial deposition
WDM	Wavelength Division Multiplexing
WDMA	Wavelength Division Multiple Access
XPM	Cross Phase Modulation

CHAPTER 1

Introduction

1.1 Fiber Optic Communication – State-of-Art

The traffic load on telecommunication links has been increasing tremendously during the last few years. Especially due to the internet with its exponentially growing number of participants all over the world and more and more multimedia applications, a further increase in line capacity is one of the major tasks for telecommunication engineers and scientists. This high transmission capacity can only be achieved by optical fibers.

Particularly, optical fiber communication plays a vital role in the development of high quality and high-speed telecommunication systems. Fiber optic communication is a way of exchanging the information between two places by sending the light signal through the optical fiber cable. Fiber optic communication brought the revolutionary change in the telecommunication industry and played a major role in the advent of information age. In the twenty first century, its advantages over electrical transmission cause the replacement of copper wire with the optical fiber in the communication system. Now the optical fiber is the most common type of channel used in communication system. Today, optical fibers are not only used in telecommunication links but also used in the Internet, local and metropolitan area networks (LAN, MAN) to achieve high signaling rates. The core advantages of optical fiber such as low loss, which allows long distances between amplifiers and its high data carrying capacity as that of thousands of electrical links would be required to carry that much data. Also no cross talk introduces in optical fibers running alongside each other for long distances as introduces in some types of electrical transmission lines.

In recent years, research interests are highly concentrated in all-optical fiber-based access networks to meet the future demand of high-speed and high-performance communications [1]. Communication capacity can be enhanced dramatically by optical networks employing multiple access techniques that allow multiple users to share the huge bandwidth of fiber optic waveguide. There are two major multiple access approaches: each user is allocated a specific time slot in time-division multiple-access (TDMA), or a specific frequency (wavelength) slot in wavelength division multiple-access (WDMA). Both techniques have

been extensively explored and utilized in optical communication systems [2-7]. Alternatively, optical code-division multiple-access (OCDMA) [8-28] is increasing attention due to its potential for enhanced information security, simplified and decentralized network control, improved spectral efficiency, and increased flexibility in the granularity of bandwidth that can be provisioned. In OCDMA, different users whose signals may be overlapped both in time and frequency share a common communications medium; multiple-access is achieved by assigning unlike minimally interfering code sequences to different transmitters, which must subsequently be detected in the presence of multiple access interference (MAI) from other users.

Optical CDMA had the potential to generate some of the previously unused bandwidth of the optical fiber and to carry over to the optical domain the benefits of CDMA in radio frequency systems. The early attempts of implementing of optical CDMA were not so successful. At that time technology available was not so advanced. In the last 20 years the optical CDMA field has matured substantially.

Although OCDMA system provides us many attractive features, but it system performances are limited due to various system impairments caused by fiber optic waveguide itself. The main problems are dispersion-induced effects which severely degrades the system performance when short duration chips are transmitted through the fiber optic waveguide. Among the various dispersion mechanisms fiber group velocity dispersion (GVD) and polarization mode dispersion (PMD) are the key limiting factors particularly in OCDMA system, as short duration chips are transmitted in the system.

1.2 Related Work and Motivation

The optical code division multiple access (OCDMA) has received significant attention in recent years because of its several attractions such as asynchronous multiple users access, privacy and security in transmission [12-18]. Until now, researches on OCDMA mainly focused on intensity modulation and direct detection on-off keying OCDMA [9], pulse position modulation OCDMA [10], direct time spread OCDMA [11], spectral encoding–decoding, asynchronous phase-encoding OCDMA [14], frequency hopping (FH) OCDMA [15], and direct sequence (DS) OCDMA [16-18]. These studies were carried out [14-18] to evaluate the bit error rate (BER) performance of OCDMA considering the effect of group velocity dispersion (GVD) only. It was found that the system performance severely degrades due to interchip interference caused by dispersion-induced spreading and

overlapping of short duration chips. Consequently, transmission distance is significantly reduced due to reduction of received optical power [29], which can be increased by incorporating optical amplifiers as a repeater in the system. To the best of our knowledge, performance of DS-OCDMA has not been studied in presence of GVD compensator. It is therefore very much important to compensate the fiber optic GVD in DS-OCDMA using a suitable compensation technique.

Normally, pre-compensation, post-compensation, dispersion compensating fiber (DCF), Maczender interferometer, and fiber Bragg grating (FBG) are used to compensate fiber optic GVD in conventional optical fiber communication system [30-32]. Among them DCF gives good results but it is bulky, costly, and not easy to handle. On other hand FBG-based GVD compensator offers significant advantages such as ready integrability with all fiber optic systems, compactness and low fabrication cost [33]. In this study, a theoretical analysis is presented to investigate the BER performance of DS-OCDMA using FBG-based GVD compensator.

It is well known that the influence of polarization mode dispersion (PMD) severely degrades the BER performance of optical fiber communication at high bit rate [34-39] due to differential group delay between two principal states of polarization which causes spreading and overlapping of pulses. In case of OCDMA system, it is believed that the PMD-induced effect will degrade BER performance due to transmission of short duration chip. To best of our knowledge, there is no study on DS-OCDMA considering the effect of PMD. In this study, an analytical approach is presented to investigate the BER performance of DS-OCDMA with in-line cascaded optical amplifiers taking into account of PMD for a single mode fiber (SMF) operating at 1550 nm. Also, a theoretical approach is presented to compensate the PMD in the proposed OCDMA system model. In our analysis, super-Gaussian and Hyperbolic-Secant shaped optical orthogonal code (OOC) are used as the user address. Avalanche photodiode (APD) is used in optical correlator receiver. To compensate signal attenuation in each fiber section, erbium doped fiber amplifier (EDFA) is used. The BER performance of the proposed system is determined as a function of system parameters considering different noises associated with the system.

1.3 Objective of the Study

In the present study the main goal is to propose an analytical approach for investigating the BER performance improvement of DS-OCDMA in dispersive fiber medium operating at 1550nm. In our analysis, super-Gaussian and Hyperbolic-Secant shaped optical orthogonal code (OOC) are used as the user address. APD is used in optical correlator receiver for optoelectronic conversion. Fiber Bragg gating (FBG) and frequency advanced higher-order PMD vectors are used to compensate the GVD, and PMD, respectively.

The main objectives of this research work are to:

➤ Propose a DS-OCDMA system model with in-line cascaded optical amplifiers.

➤ Determination of system parameters for which the proposed system performance will be improved.

➤ Carry out the BER performance analysis of the proposed DS-OCDMA in presence of GVD with different chipshapes and GVD compensator:

- To find out the BER versus number of simultaneous user for different fiber lengths, and chip rates.
- To find out the BER versus received signal power for different fiber lengths, and chip rates.
- GVD-induced penalty as a function of simultaneous users, fiber lengths, chip rates, and chipshapes will be studied.
- To find out the optimum parameters of the FBG-based GVD compensator.
- Investigation of the improvement of system performance in terms of system and compensator parameters.

➤ Carry out the BER performance analysis of the proposed DS-OCDMA in presence of PMD and PMD compensation:

- To find out the BER versus number of simultaneous user for different fiber lengths, and chip rates.
- To determine the BER versus received signal power for different fiber lengths, and chip rate.
- PMD-induced penalty for different fiber lengths, and chip rates will be studied.
- To find out the BER performance improvement in presence of PMD compensations.

1.4 Outline of the Thesis

A brief introduction to communication system is presented in Chapter 1 with an emphasis on OCDMA system. This chapter is also presents the related works, motivation, and the objectives of this thesis.

Chapter 2 introduces common multiple access techniques in optical domain and also the precious spread spectrum communication methods including direct sequence and frequency hopping. An overview on OCDMA is given in this chapter. Chapter 2 is also presents the current codes that were developed throughout the recent years. This chapter is also presents linear and nonlinear phenomenon in optical fibers. It is also describing different dispersion compensation mechanism in fiber optic waveguide.

In Chapter 3 introduces the proposed OCDMA system and derive the mathematical formulas of the proposed model.

The results and discussion are presented in Chapter 4. In this chapter, we present the results for different parameters that improved the BER performance of the DS-OCDMA.

Finally, Chapter 5 concludes this thesis with future scope of works.

CHAPTER 2

Fundamental Concept

As global network infrastructures expand to support various type of traffic, photonic networks are expected to take an important rule. The increasing demand for bandwidth forces network infrastructures to be of large capacity and reconfigurable. The efficient utilization of bandwidth is a major design issue for ultrahigh-speed photonic networks. The two main techniques for multiplexing data signals are currently time division multiplexing (TDM) and wavelength division multiplexing (WDM). Optical code division multiple access (OCDMA) is an alternative method, which performs encoding and decoding through an optical signature code, in order to allow the selection of a desired signal so that different users can share the same bandwidth. In such a system, data signal overlap both in time and wavelength. The OCDMA networks have several advantages over TDMA or WDM networks, e. g. complete utilization of the entire time frequency domain by each subscriber, flexibility in network design (because the quality depends on the number of active users) and security against encryption.

The Chapter is organized as follows. Section 2.1 reviews the basic multiple access techniques in optical domain. Section 2.2, a closer look is taken at the basic fundamentals of OCDMA, potential implementation schemes are named, and advantages and disadvantages of OCDMA, and an overview on current codes are given. Section 2.3, briefly discuss the linear and nonlinear characteristics of optical fiber. Different methods of dispersion compensation in fiber optic waveguide are presented in Section 2.4.

2.1 Multiple Access Techniques

In order to make full use of the available bandwidth in optical fibers and to satisfy the bandwidth demand in future networks, it is necessary to multiplex low-rate data streams onto optical fiber to accommodate great number of subscribers. There is a need for technologies that allow multiple users to share the same frequency, especially as wireless telecommunications continues to increase in popularity. Currently, there are three common types of multiple access systems:

• Wavelength division multiple access (WDMA)

• Time division multiple access (TDMA)

• Code division multiple access (CDMA)

2.1.1 Wavelength Division Multiple Access (WDMA)

In WDMA system, each channel occupies a narrow optical bandwidth (≥ 100 GHz) around a centre wavelength or frequency [3].
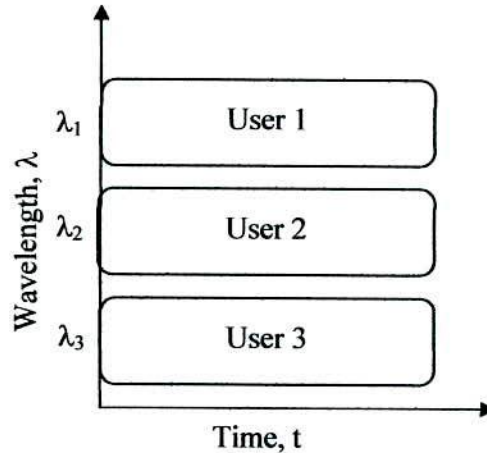
Fig. 2.1: *Resource sharing based on WDMA technique.*

The modulation format and speed at each wavelength can be independent of those of other channels as shown in Fig. 2.1. Arrayed or tuneable lasers will be needed for WDMA applications [6]. Because each channel is transmitted at a different wavelength, they can be selected using an optical filter [5]. Tuneable filters can be realized using acousto-optics [40], liquid crystal [42], or fiber Bragg grating [33]. To increase the capacity of the fiber link using WDMA we need to use more carriers or wavelengths, and this requires optical amplifiers [41] and filters to operate over extended wavelength ranges. Due to greater number of channels and larger optical power the increased nonlinear effects in fibers causes optical crosstalk such as four wave mixing [43] over wide spectral ranges. Another approach to increase the capacity of WDMA links is to use dense WDM (DWDM) [7], which will have to operate with reduced channel spacing (ITU-T recommendation G.692 defines 43 wavelength channels from 1530-1565 nm, with a spacing of 100 GHz). This requires a sharp optical filter with linear phase response, wavelength stable components, and optical amplifiers with flat gain over wide bandwidths, and optical fibers must support hundreds of channels without distortion or crosstalk. With respect to channel switching, wavelength routing is the next switching dimension for DWDM, with interferometric

crosstalk being an essential issue in the implementation of cross connects based on space and wavelength [44]. Hence, the extent of wavelength routing that is realizable places fundamental limits on network flexibility, which in turn determines switch size and implementations complexity and costs.

2.1.2 Time Division Multiple Access (TDMA)

In TDMA system, each channel occupies a pre-assigned time slot, which interleaves with the time slots of other channels as shown in Fig. 2.2.
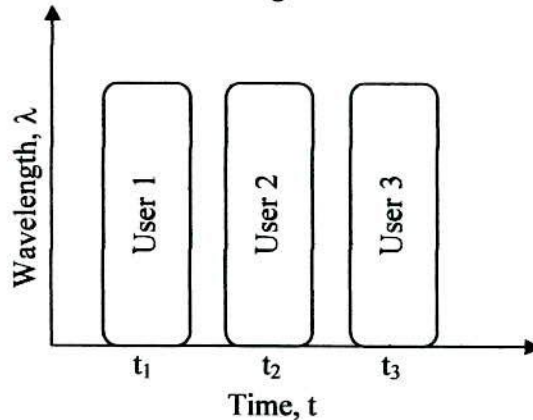
Fig. 2.2: Resource sharing based on TDMA technique.

Synchronous digital hierarchy (SDH) is the current transmission and multiplexing standard for high-speed signals, which is based on time division multiplexing [45]. Optical TDMA (OTDMA) networks can be based on a broadcast topology or incorporate optical switching. In broadcast networks, there is no routing or switching within the network. Switching occurs only at the periphery of the network by means of tuneable transmitters and receivers. The switch-based networks perform switching functions optically within the network in order to provide packet-switched services at very high bit-rates [46-47]. In an electrically time-multiplexed system, multiplexing is carried out in the electrical domain, before the electrical-to-optical conversion (E/O) and demultiplexing is performed after optical-to-electrical conversion (O/E). Major electronic bottlenecks occur in the multiplexer E/O, and the demultiplexer O/E, where electronics must operate at the full multiplexed bit-rate. Alternatively, in optically time-multiplexed systems where by moving the E/O and O/E converters to the baseband channels the electronic bottlenecks are alleviated [2]. OTDMA systems offer a large number of node addresses; however, the performance of OTDMA systems is ultimately limited by the time-serial nature of the

technology. OTDMA systems also require strong centralized control to allocate time slots and to manage the network operation.

2.1.3 Code Division Multiple Access (CDMA)

CDMA is one of a family of transmission techniques generically called spread spectrum, explained in the following section. In this technique, the network resources are share among users which are assigned a code instead of time slot like TDMA or a wavelength like WDMA. Then, users are capable of accessing the resources using the same channel at the same time, as shown in the Fig. 2.3. The concepts of spread spectrum i.e. CDMA seem to contradict normal intuition, since in most communications systems try to maximize the amount of useful signal with a minimal bandwidth.
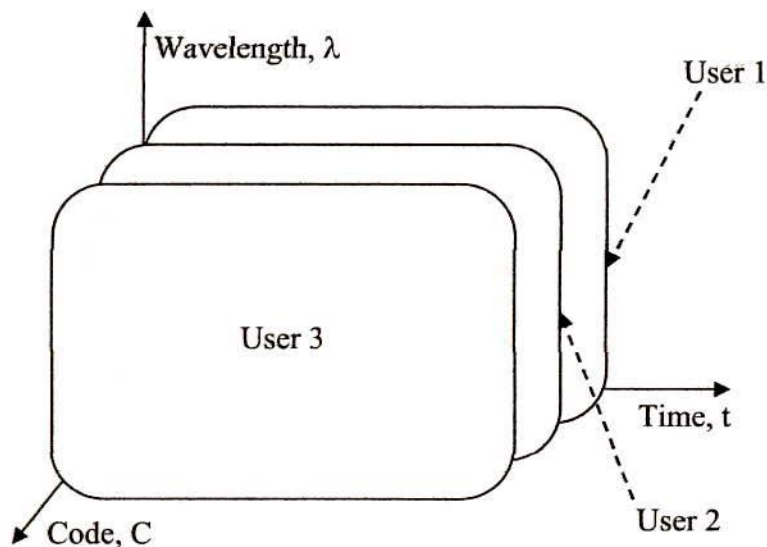
Fig. 2.3: Resource sharing based on CDMA technique.

In CDMA we transmit multiple signals over the same frequency band, using the same modulation techniques at the same time.

2.2 Characteristics of OCDMA

The CDMA technique has its origin in the spread spectrum (SS) technique. SS has been developed in the 1940's as military radio application which offers high security transmission. In an SS transmission, the input signal is coded in such a way, that its spectrum spreads over a much wider range than the original signal. At the receiver, the spreaded signal is decoded and its original form is restored. While despreading the input signal, unwanted noise or intentional jamming signals are spreaded, i.e. though input

signal and distortion might carry the same power, the power spectral density of the distortion covers a wider area, thus enabling the receiver to detect the input signal and noticing some additional, but only weak noise (see Fig. 2.4). Furthermore, a despreading of the input signal is impossible without exact knowledge of the code sequence, thus increasing the security of the transmission.
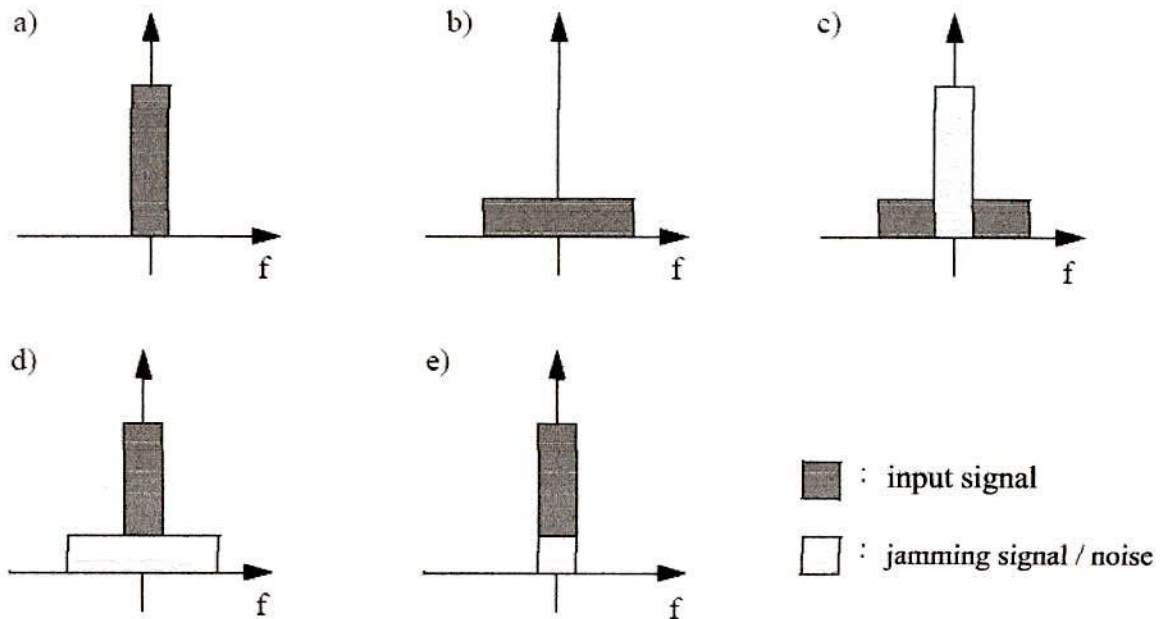
Fig. 2.4: Principle of spread spectrum communication: a) Spectrum of input signal. b) Spectrum of coded input signal (to be transmitted). c) Jamming signal/noise overlapping input signal during transmission. d) Decoded signal, input signal is compressed; jamming signal/noise is spreaded. e) Filtered signal at receiver, input signal can be detected.

If each of the users is assigned to its own code sequence which is orthogonal to all others, they can all access the transmission medium at the same time at the same carrier frequency, resulting in the so-called CDMA. CDMA has been of high attractiveness as multiple access scheme in radio applications because of

- non-sensitivity against narrow-band jamming signals

- *efficient use of transmission medium in bursty traffic scenarios*

- high security due to coded transmission.

In fiber optic applications, these first-sight advantages are less interesting. Narrow-band jamming signals are not to be expected on a fiber link, traffic is, if not in local area networks, rather of continuous nature than of bursty. Still, OCDMA can be of interest. Again, in LAN applications with bursty traffic environment, CDMA is a first choice multiple access scheme due to low coordination necessary between different users. Whereas in TDMA schemes, all users are assigned to fix time frames or, in WDMA schemes, to fix wavelength, this is not the case in CDMA transmission. In case of temporal or spectral overlapping, system performance decreases immediately in pure TDMA/WDMA applications.

Several methods have been developed for coding, two of them have come into closer focus during the recent years:

- Direct sequence (DS) CDMA, a temporal coding technique. Each mark of the input bit sequence is encoded into a whole sequence of marks and spaces (the code sequence, also called chip sequence), each space is encoded into another orthogonal code sequence. In case of unipolar environment as is in fiber optic transmission, a space is not encoded, since a space carries no energy. Thus, there is no signal in that time slot that can be encoded.

- Frequency hop (FH) CDMA, a spectral coding technique. The carrier frequency is shifted periodically according to a certain, pre-assigned code. All channels share the entire bandwidth by using different carrier wavelengths at different times according to a certain code. Since FH CDMA requires tuneable laser sources for optic applications or the creation of a supercontinuum with subsequent filtering [48-50], this CDMA scheme has not been further taken into consideration in this work, because one of the aims of this work has been the improvement of system performance without extending the system's complexity.

The different potential applications for a CDMA system are

- Local area and broadcast networks
- High bit rate point-to-point links
- *Robust and secure transmission*

2.2.1 Advantages of OCDMA

Some of the main advantages of using OCDMA systems can be summarized as follows:

• Equal distribution of available bandwidth.

• Control and organization of the network.

• Provisioning of value-added services.

• Security.

Bandwidth: In OCDMA, users can access equal portions of the available channel bandwidth. Here, the bandwidth is equally shared by all active users and can be divided into virtual channels. Consequently, the OCDMA system users can equally share access of the available resources of the network. Further, this is also the reason why, no single user one can block another from accessing the optical channel, one major advantage of OCDMA networks.

Network Control: In OCDMA technology, the optical codes of optical are distributed in such a way that, the peak auto correlation for the shifted and non shifted optical signals can be alternatively small or large. Consequently, the optical receivers can manipulate asynchronously these signals without the need of global clock synchronization between them. In this way, the OCDMA technology can properly manipulate and control the signal transmitted within the whole system.

Value added Services: In OCDMA uses different types of optical codes. In this way, various services for different types of traffic can be easily introduced. For example, the code rate for high and low importance traffic can be set different such that transfer of e.g., real time audio/video signals and electronic mail can be give different priorities. Consequently, OCDMA plays an important role in providing customized or value-added services to its users.

Security: If we consider an OCDMA system with 41 wavelengths and 961 time chips, it will require 1350 years trying all possible combinations before the code could be broken.

Meanwhile, in one second, the OCDMA system can have more than 107 such codes are used. For this reason, the security of the OCDMA system is inherent within the OCDMA technology, which is a major advantage of OCDMA-enabled networks.

2.2.2 Drawbacks of OCDMA

In spite of their many advantages, OCDMA systems suffer from several drawbacks which may be summarized as follows:

• Noise.

• Error correction.

• Encoding/Decoding.

• Security integration.

Noise: Beat and shot noise are both technological barriers of the physical channel which degrade the performance of the OCDMA network. Beat and shot noise are not appearing *on the same wavelengths in case of multiple accesses. This is why, for a fixed receiver, the* energy is used for a single channel wavelength. On the other hand in OCDMA systems, the total bandwidth is distributed.

That's why beat and shot noise may be introduced in the wavelengths of the same transmission channel. In OCDMA with the same wavelengths the channel bandwidth is allocated which is the optical power from other user which guide the shot noise.

Shot noise is defined as the optical root square of the received power and is direct proportional to the number of users. This type of noise reduces the scalability of the OCDMA network.

Error Correction: Forward error correction is costly and unusable in OCDMA because the speed for carrying the information in electrical cables and optical fiber is not same. For this reason, we have to design specialized encoding and/or decoding devices in order to correct the errors in case of optical signal transmissions.

It is possible to design codes for forward error correction devices which exclusively depend on optical signal processing, such as optical multiplexing and wavelength shifting.

As a result of such codes, we can manage error free transmissions in case of optical signal processing.

Encoding/Decoding: The optical signal follows two dimensional codes. Fiber Bragg Grating (FBG) is a periodic perturbation of the refractive index along the fiber length which is formed by exposure of the core to an intense optical interference pattern [33]. The optical encoder supports FBG and has a predefined center frequency and temperature. For this reason a wavelength control loops or robust encoding device is required in order to ease this effect.

Security Integration: Integration of hybrid laser technology represents a monetary cost barrier in optical communication technologies. As a waveguide based encoder and as a waveguide modulator, an array of tunable lasers integrated on the same substrate. Substrate refers to the manufacturing materials. Semiconductor devices are manufactured from this material. Consequently, a waveguide modulator and demodulator are cheaper to manufacture than a monolithic LASER integration.

2.2.3 Current codes

The following sections deal with the most important codes for DS-OCDMA. Codes for a bipolar transmission have not been considered due to the necessary complex transmitter and receiver structure as explained earlier. Common to all codes is the ability to extract a user's code, also called signature sequence, in the presence of other user's signature sequences. A set of signature sequences for which any two signature sequences are easily distinguishable from a possibly time-shifted version of each other is needed. Strict orthogonality between different codewords would require $\rho_a = \rho_c = 0$. Due to the positive nature of an intensity-modulated, direct-detection system, this cannot be met. This is one of the starting points for the different code families in sections 2.2.3.1 to 2.2.3.3. All code families should fulfill the following points:

- Minimization of code word length F. The shorter the codeword, the lower the chip rate B_c, thus higher bit rates B_b can be coded before running into problems with electronic component speeds.

- Maximization of code weight w. w equals the peak value of the ACF. The higher this peak, the better the SNR.

- Minimization of ρ_a. The lower the value of ρ_a, the more resembles the ACF a clear and distinct peak. Important for easy tracking and synchronization.

- Minimization of ρ_c. The lower the value of ρ_c, the more users can simultaneously transmit, since the overall interference is limited by $K \cdot \rho_c$, K being the number of simultaneous users. Error-free detection is possible if $n \cdot \rho_c < w$.

- Maximization of code size $|C|$ being identical to the number of possible codewords N Maximization of possible simultaneous code words, which must not necessarily be equal to $|C|$.

Generally, these conditions cannnot be met at the same time and compromises have to be found. The conventional codes in sections 2.2.3.1 to 2.2.3.3 emphasize different requirements of those mentioned above.

2.2.3.1 Optical orthogonal codes

An optical orthogonal code (OOC) is characterized by the quadruple (F, w, ρ_a, ρ_c) with $\rho_a = \rho_c = 1$. All codewords of an OOC have length and weight (number of marks) w. An OOC can be constructed by using a variety of methods [51] such as iterative construction methods, the Greedy algorithm, algebraic coding theory, techniques with the help of projective geometry or set theory. By stipulating code word length F and code weight w, the appropriate OOC's are found by optimizing the relative delays between the chips within a codeword with respect to the other codewords [22]. It follows that for given F and w, a maximum N of possible OOC can be constructed with

$$N \leq \left[\frac{F-1}{w(w-1)} \right] \tag{2.1}$$

where the brackets denote the integer portion of the real value. An upper bound on the BER can be found by assuming a chip synchronous overlap of the codewords (worst case). To derive the BER of OOC's, it is first necessary to determine the probability density function (pdf) of one mark in a codeword to overlap with a mark in another codeword.

Since there are $w \cdot w$ possibilities for the marks in the codewords to overlap and the probability of each individual overlap is $1/F$, the probability of an overlap is

$$p = \frac{w^2}{F} \tag{2.2}$$

The pdf of the event of overlap k can then be derived as

$$p_k(k) = (1 - \frac{w^2}{F})\delta(k) + \frac{w^2}{F}\delta(k-1) \tag{2.3}$$

δ being Dirac's delta distribution. Considering the on-off modulation of the bit sequence that has to be encoded, a random variable $u = \frac{1}{2}k$ can be defined, since the bit sequence contains marks and spaces with equal probability. It follows that

$$P_u(u) = (1 - \frac{w^2}{2F})\delta(u) + \frac{w^2}{2F}\delta(u-1) \tag{2.4}$$

To drive the BER, it is now necessary to determine the pdf for the interference. One obtains

$$P_I(I) = \sum_{i=0}^{N-1} \binom{N-1}{i} \left(\frac{w^2}{2F}\right)^i \left(1 - \frac{w^2}{2F}\right)^{N-1-i} \delta(I-1) \tag{2.5}$$

The BER can thus be obtained by

$$BER = \frac{1}{2} \sum_{i=Th}^{N-1} \binom{N-1}{i} \left(\frac{w^2}{2F}\right)^i \left(1 - \frac{w^2}{2F}\right)^{N-1-i} \tag{2.6}$$

Equation (2.6) is the upper bound for the BER, since it assumes a chip synchronized transmission where Th is the threshold value.

2.2.3.2 Prime sequence codes

Prime sequence (PS) codes can also be characterized by a quadruple (F, w, ρ_a, ρ_c) with $\rho_a = w-1$ and $\rho_c = 2$. All codewords have the same weight w, where $w = P$, P being a prime number. The code word length equals F with $F = P^2$. PS code words are constructed by using the multiplication table of the elements of the Galois Field GF (P) [52]. Codewords are divided into P time frames. By this, the distances between marks within a codeword

are different for different sequences and every time frame contains only one mark. Each family of PS code words thus contains exactly

$$N = P \qquad (2.7)$$

different codewords. The BER can be Gaussian approximated by using the central limit theorem and follows as

$$BER = \Phi\left(\frac{-P}{\sqrt{1.16 \cdot (N-1)}}\right) \qquad (2.8)$$

With N being the number of simultaneous users and $\Phi(x)$ is the unit normal cumulative distribution function

$$\Phi(x) = \frac{1}{\sqrt{2\pi}} \int_{-\infty}^{x} e^{-\frac{y^2}{2}} dy \qquad (2.9)$$

2.2.3.3 Quadratic congruence codes

Quadratic congruence (QC) codes are developed with the help of the number theoretic concept [53]. They can also be characterized by a quadruple (F, w, ρ_a, ρ_c), where $F = P^2$ denotes the code word length, $w = P$ the code weight, P being a prime number, the ACF constraint $\rho_a = 2$, and the CCF constraint $\rho_c = 2$. Similar to PS codes, there are exactly $N = P$ different code words within a code family for a specified prime number P. Superior to PS codes, their ACF constraint enables their use in fully asynchronous environments. Their ACF's are almost ideal in a sense of optical codes at the expense of having slightly increased number of coincidences.

The BER can, similar to the BER of PS codes, be computed by [53]

$$BER = \Phi\left(\frac{-P}{\sqrt{1.78 \cdot (N-1)}}\right) \qquad (2.10)$$

with N being the number of simultaneous users and $\Phi(x)$ the unit normal cumulative distribution function. The most important advantage of QC codes lies in the much lower side lobes of the ACF, so that tracking and synchronization to the transmitter is much easier due to the sharp peak in the ACF. The higher number of coincidences in the CCF ($\rho_c = 4$) leads to higher interference and a worse BER compared to PS codes ($\rho_c = 2$).

In our present study, Optical Orthogonal Codes (OOC) is used. Because it is incoherent optical codes extensively used [23], since they can be easily generated and processed using planar lightwave circuit (PLC) devices.

2.3 Characteristics of Optical Fiber

The characteristics of optical fibers are divided into two main categories, namely linear and nonlinear.

2.3.1 Linear Characteristics

The main linear characteristics of optical fibers are: attenuation, group velocity dispersion, polarization mode dispersion and optical SNR.

2.3.1.1 Attenuation

Coupling losses between the source/fiber, fiber/fiber and fiber/detector can cause attenuation in optical links. The attenuation/wavelength characteristic of a typical glass fiber is shown in Fig. 2.5. This figure also shows the relative magnitudes of the four main sources of attenuation: electron absorption, Rayleigh scattering, material absorption and impurity absorption. The first three of these are known as intrinsic absorption mechanisms because they are characteristic of the glass itself. Absorption by impurities is an extrinsic absorption mechanism.
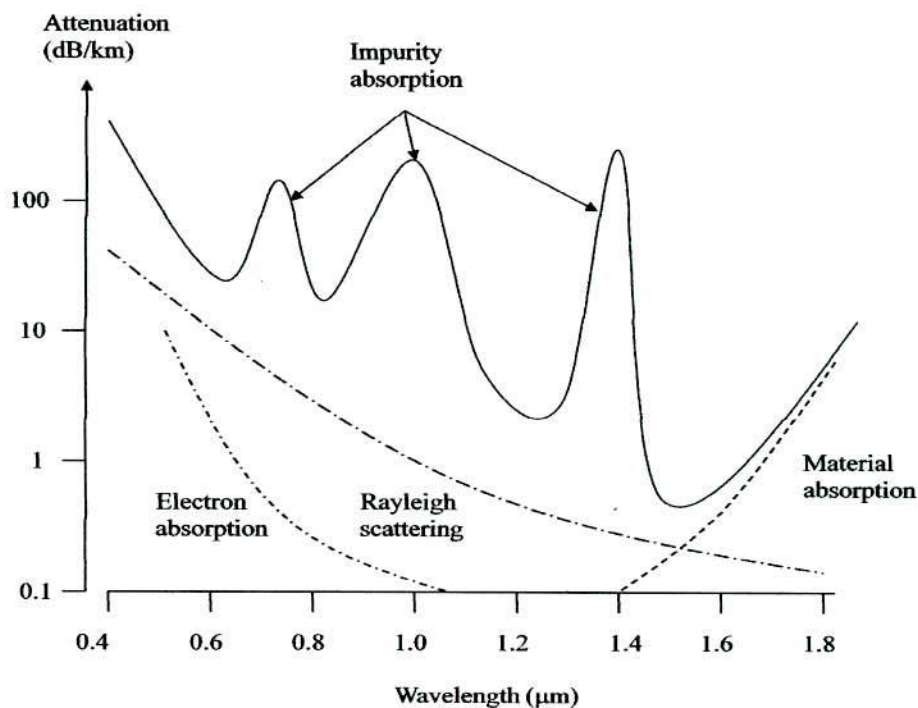
Fig. 2.5: Attenuation/wavelength characteristic of a silica-based glass fiber.

Impurity absorption: In ordinary glass, impurities, such as water and transition metal ions, dominate the attenuation characteristic. However, because the glass is usually thin, the attenuation is not of great concern. In optical fibers that are several kilometers long, the presence of any impurities results in very high attenuations which may render the fiber useless; a fiber made of the glass used in lenses would have a loss of several thousand dB per km. By contrast, if we produced a window out of the glass used in the best optical fibers, then we would be able to see through a window 30 km thick.

The presence of water molecules can dominate the extrinsic loss. The OH bond absorbs light at a fundamental wavelength of about 2.7 μm and this, together with interactions from silicon resonances, causes harmonic peaks at 1.4 μm, 950 nm and 725 nm. Between these peaks are regions of low attenuation - the transmission windows at 850 nm, 1.3 μm and 1.55 μm. As a large water concentration results in the tails associated with the peaks being large, it is important to minimize the OH impurity concentration.

In order to reduce attenuation to below 20 dB/km, a water concentration of less than a few parts per billion (p.p.b.) is required. Such values are being routinely achieved by using the modified chemical vapour deposition manufacturing process. Different manufacturing methods will produce lower water concentrations. For example, the vapour-phase axial deposition, VAD, process can produce fibers with OH concentrations of less than 0.8 ppb. With this impurity level, the peaks and valleys in the attenuation curve are smoothed out, and this results in a typical loss of less than 0.2 dB/km.

The presence of transition metal ions (iron, cobalt, copper, etc.) can cause additional loss. If these metals are present in concentrations of 1 ppb, then the attenuation will increase by about 1 dB/km. In telecommunications-grade fiber, the loss due to transition metal ion impurities is usually insignificant in comparison with the OH loss.

Rayleigh scattering: Rayleigh scattering results from the scattering of light by small irregularities in the structure of the core. These irregularities are usually due to density fluctuations which were frozen into the glass at manufacture. Consequently this is a fundamental loss mechanism, which places a lower bound on the fiber attenuation. Rayleigh scattering is only significant when the wavelength of the light is of the same order as the dimensions of the scattering mechanism. In practice, this loss reduces as the fourth power of wavelength, and so operation at long wavelengths is desirable.

Material absorption: The atomic bonds associated with the core material will absorb the long wavelength light is called material absorption. Although the fundamental wavelengths

of the absorption bonds arc outside the range of interest, the tails are significant. Thus operation at wavelengths greater than 1.55 μm will not produce a significant drop in attenuation.

Electron absorption: In the ultra-violet region, light is absorbed by photons exciting the electrons in a core atom, to a higher energy state. In silica fibers, the absorption peak occurs in the ultra-violet region at about 0.14μm; however, the tail of this peak extends through to about 1 μm, so causing attenuation in the transmission windows.

2.3.1.2 Group Velocity Dispersion (GVD)

There are several reasons for the reduced performance of optical fiber communications. Group velocity dispersion is such an effect which can reduce the performance of passive optical networks.

Group velocity dispersion is the combinations of mainly two factors: dispersion of material and dispersion of the waveguide. GVD is the effect of pulse spreading (or broadening) and can reduce the integrity of a received signal unless appropriate dispersion modules are included in the optical communication system.

Material Dispersion: This type of dispersion results from the fact that the refractive index of the fiber medium varies as a function of wavelength. This causes a wavelength dependence of the group velocity of any given mode; that is, pulse spreading occurs even when different wavelengths follow the same path.
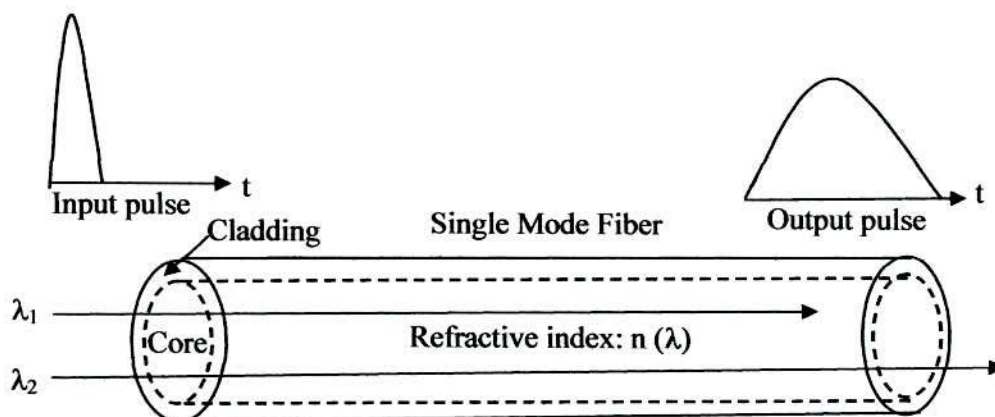
Fig. 2.6: Material Dispersion.

Wave-guide Dispersion: Wave-guide dispersion is very similar to material dispersion in that they both cause signals of different wavelengths and frequencies to separate from the

light pulse. However, wave-guide dispersion depends on the shape, design, and chemical composition of the fiber core. Only 80 percent of the power from a light source is confined to the core in a standard single-mode fiber, while the other 20 percent actually propagates through the inner layer of the cladding. This 20 percent travels at a faster velocity because the refractive index of the cladding is lower than that of the core. Consequently, signals of differing frequencies and wavelengths are dispersed and the pulse becomes indistinguishable. An increase in the wave-guide dispersion in an optical fiber can be used in order to counterbalance material dispersion and shift the wavelength of zero chromatic dispersion to 1550 nm.
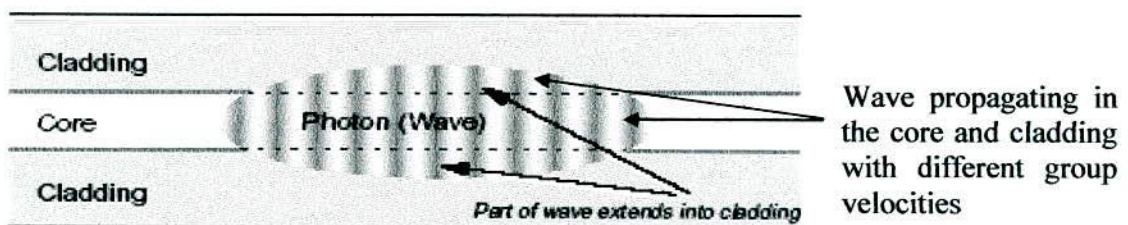
Fig. 2.7: Waveguide Dispersion.

2.3.1.3 Polarization Mode Dispersion

The polarization related impairments have become a major obstacle to the increase transmission rates in optical fiber communication systems. Such impairments include polarization mode dispersion (PMD) in optical fibers, polarization-dependent loss (PDL) in passive optical components, polarization-dependent modulation (PDM) in electro optical modulators, and polarization-dependent gain (PDG) in optical amplifiers. Polarization Mode Dispersion is an important linear phenomenon occurring inside optical fibers, which can cause the optical receiver to be unable to interpret the signal correctly, and results in high bit error rates. PMD can dramatically decrease the fiber optic network's performance, particularly those networks operating at high data rates. It can distort signals, render bits inaccurate, and destroy the signal integrity of the network.

While the phenomenon of PMD has been known for years, it has only been recently that it has posed a serious, realistic problem for optical networks. PMD's negative effects result in a limitation of a networks bandwidth or length that is, of course, undesirable. It is important to understand however, that with proper measurement and management, the negative effects of PMD may be minimized or eliminated altogether.

The older fibers had the PMD value 100 times greater than that of the present day fibers. But in the new fiber the PMD remains the major problem because of the following reasons [54, 55]:

a) *There is still a small residual asymmetry in the fiber core as shown in Fig. 2.8.*

b) Slight PMD exists in the line components such as isolators, couplers, Erbium Doped Fibers, modulators and multiplexers.

Perfect   Oval   Stress
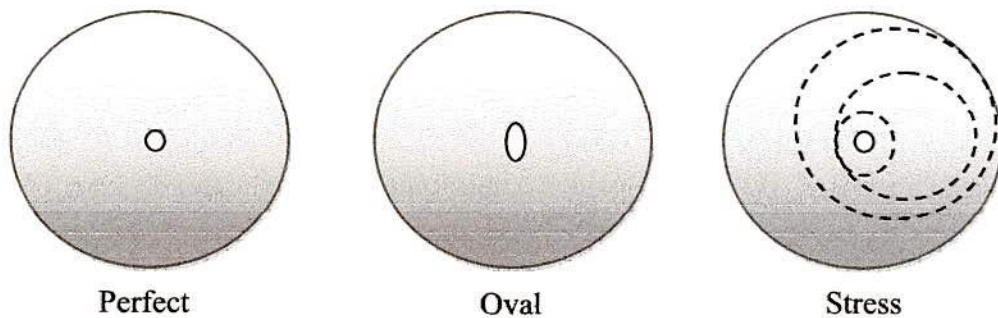
Fig. 2.8: Cross-sectional defects of optical fibers.

In addition to this, internal forces induced by thermal expansion and external forces induced by the environment through handling and cabling, such as bending and twisting, add slight nonsymmetrical stress fields inside the fiber core. These deviations give rise to the phenomenon of birefringence. As a result of a property of optical fibers called 'birefringence', different polarizations of light are propagated at different velocities through the fiber. As laser light is generally highly polarized, the digital bits that they emit contain light that is also highly polarized. Couple this with the birefringence present in the fiber and the result is that different components (polarizations) of the digital bits travel at different velocities [56]. In other words some of the light in the bit travels faster and some of the light travels slower. This causes the digital bit to spread in time; this is termed dispersion. Moreover, the residual birefringence is not constant along the length of the fiber but changes with distance in a random way, not only in amount, but also in its local principal axes. So in the best conditions, PMD still significantly limits the deployment of high bit rate systems. For a given fiber, PMD is supposed to be fixed. However, this is not the case in real communication systems because environment fluctuations cause PMD to vary randomly in time. Therefore, it is important to understand the statistical properties of pulse propagation induced by PMD.

Single-mode optical fiber and components support one fundamental mode, which consists of two orthogonal polarization modes. This asymmetrical stress field introduces small refractive index differences for the two polarization states. This characteristic is known as birefringence. The birefringence causes one polarization mode to travel faster than the other, resulting in a difference in the propagation time, which is called the differential group delay (DGD). DGD is the unit that is used to describe PMD. DGD is typically measured in picoseconds. A fiber that acquires birefringence causes a propagating pulse to lose the balance between the polarization components. This leads to a stage in which different polarization components travel at different velocities, creating a pulse spread as shown in Fig. 2.9. PMD can be classified as first-order PMD, also known as DGD, and second-order PMD (SOPMD). The SOPMD results from dispersion that occurs because of the signal's wavelength dependence and spectral width. If the fibers were perfect, the state of polarization (SOP) of the light signal transmitting in the fiber would remain constant and the effects of the PMD, PDL, PDM, and PDG could be easily eliminated.
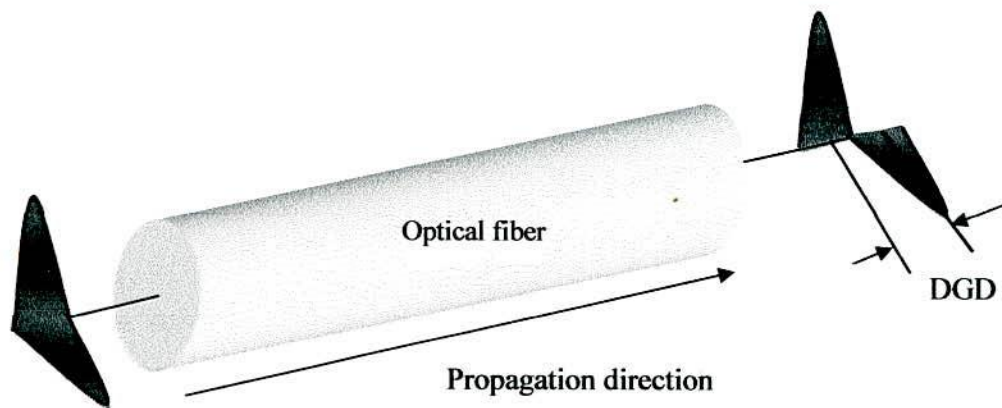
Fig. 2.9: Polarization Mode Dispersion.

Unfortunately, the SOP of light propagating in the length of communication fiber varies along the fiber due to random birefringence induced by the thermal stress, mechanical stress, and irregularities of the fiber core. Generally, at the output end of fiber the light polarized, with varying degrees of ellipticity, and with the major elliptical axis at the arbitrary angle. Worst of all, the induced birefringence changes with temperature, pressure, stress and other environmental variations, making polarization impairments time dependent. The single mode fibers manufactured in mid 1990s have the property that has become more problematic as the bit rates and span lengths increases. This all was due to the imperfectly rounded fiber core. As the core of a fiber should have a perfect cylindrical shape, but in practice it is not possible to have ideally cylindrical shape because of change

in core diameter randomly while drawing the fiber, so because of this physical limitation the PMD occurs [47]. So as it is impossible to manufacture the perfectly symmetrical and rounded fiber, the researchers got success to produce more symmetrically rounded fiber. But the problem of PMD still exists with a small coefficient of 0.5 $ps/\sqrt{Km}$ [35, 57].

PMD is not an issue at low bit rates but becomes an issue at bit rates in excess of 10 Gbps. PMD is noticeable at high bit rates and is a significant source of impairment for ultra-long-haul systems. PMD compensation can be achieved by using PMD compensators that contain dispersion-maintaining fibers with degrees of birefringence in them. The introduced birefringence negates the effects of PMD over a length of transmission. For error-free transmission, PMD compensation is a useful technique for long-haul and metropolitan-area networks running at bit rates greater than 10 Gbps. The PMD value of the fiber is the mean value over time or frequency of the DGD and is represented as $ps/\sqrt{Km}$.

2.3.2 Non Linear Characteristics

In this section we will try to differentiate between several nonlinearities, both elastic and inelastic and as a result, the energy is exchanged in the medium. The major non linear characteristics in optical fibers are as follows: Cross phase modulation, Self phase modulation, and Four-wave mixing.

Self Phase Modulation (SPM): Phase modulation of an optical signal by itself is known as self-phase modulation (SPM). SPM is primarily due to the self-modulation of the pulses. Generally, SPM occurs in single-wavelength systems. At high bit rates however, SPM tends to cancel dispersion. However, consideration must be given to receiver *saturation and to nonlinear effects such as SPM, which occurs with high signal levels.* SPM results in phase shift and a nonlinear pulse spread. As the pulses spread, they tend to overlap and are no longer distinguishable by the receiver. The acceptable norm in system design to counter the SPM effect is to take into account a power penalty that can be assumed equal to the negative effect posed by XPM. By the SPM-impact new spectral components are generated in the optical signal spectrum resulting in a spectral broadening.

Cross Phase Modulation (XPM): Cross-phase modulation (XPM) is a nonlinear effect that limits system performance in wavelength Division Multiplexed (WDM) systems.

XPM is the phase modulation of a signal caused by an adjacent signal within the same fiber. XPM is related to the combination (dispersion/effective area). XPM results from the different carrier frequencies of independent channels, including the associated phase shifts on one another. The induced phase shift is due to the walkover effect, whereby two pulses at different bit rates or with different group velocities walk across each other. As a result, the slower pulse sees the walkover and induces a phase shift. The total phase shift depends on the net power of all the channels and on the bit output of the channels. Maximum phase shift is produced when bits belonging to high-powered adjacent channels walk across each other.

Four Wave Mixing (FWM): FWM can be compared to the inter-modulation distortion in standard electrical systems. When three wavelengths (λ_1, λ_2, λ_3) interact in a nonlinear medium, they give rise to a fourth wavelength (λ_4), which is formed by the scattering of the three incident photons, producing the fourth photon. This effect is known as four-wave mixing (FWM) and is a fiber-optic characteristic that affects WDM systems. The effects of FWM are pronounced with decreased channel spacing of wavelengths and at high signal power levels. High group velocity dispersion also increases FWM effects. FWM also causes interchannel cross-talk effects for equally spaced WDM channels.

2.4 Dispersion compensation in fiber optic waveguide

Depending on the place and realization where the dispersion compensation is made in a system, compensating methods are classified as: a) pre-chirp techniques at the transmitter side b) dispersion compensation in the transmission line (inline compensation) and c) dispersion compensation at the receiver side (Fig. 2.10).
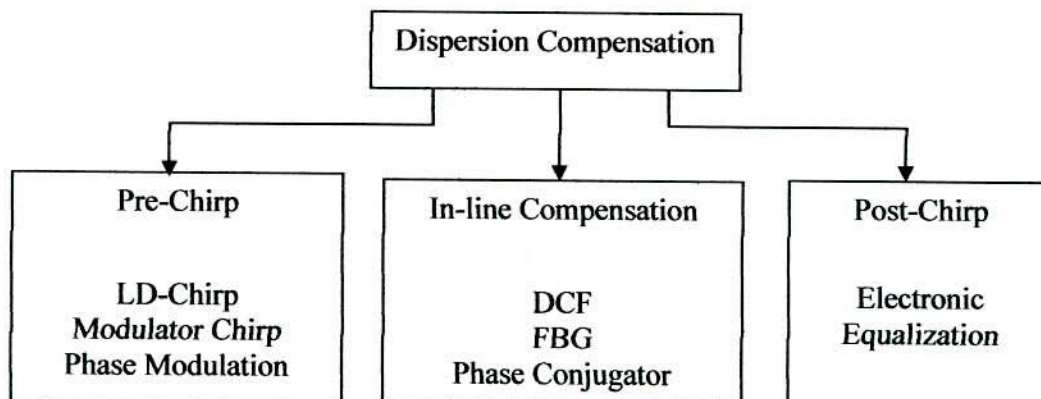

Fig. 2.10: Dispersion compensation methods.

The idea behind the pre-chirping at the transmitter side is the implementation of chirp with the opposite sign to the fiber chirp in order to counter the GVD effects in the fiber. The main implementation area of this technique is cost effective, optical short-reach systems (e.g. MANs) with smaller channel bit rates, but in combination with other dispersion compensation techniques (e.g. in-line compensation) it can enable a performance improvement even in high-bit rate transmission systems over long distances [59]. The post-chirp techniques at the receiver side are characterized by the compensation of the group velocity dispersion in electrical domain. This compensation method is cost effective, and in combination with in-line compensation, enables an enhanced transmission performance. In-line dispersion compensation represents the key enabling technology for the realization of long-haul transmission systems. The dispersion compensation is realized in the optical domain without electro-optical conversion of the signal, enabling better compensation of the signal because the optical phase is maintained. The following dispersion compensating devices are used for the realization of in-line dispersion compensation:

Dispersion Compensating Fiber (DCF) represents the most widely used in-line dispersion compensation technique in today's transmission systems. The DCFs are characterized by a large negative dispersion and a small core diameter. The large negative dispersion values can be achieved by variation of doping the fiber cladding (e.g. by fluorine), *introducing an increase in the refractive index difference between the core and cladding.* The demands on DCFs are a large negative dispersion (-70-300 ps/nm), low insertion losses, low polarization dependent (PDL) losses, a low polarization mode dispersion (< 0.05 ps/√km), a large effective area (A_{eff}) and a negative dispersion slope. The DCFs can be used for simultaneous compensation of several channels, but due to imperfections in slope compensation, a small amount of residual dispersion remains especially in outer channels.

Phase Conjugator is utilizes the concept known as mid-span spectral inversion (MSSI). The principle of MSSI is the spectral inversion of the optical signal spectrum in the middle of the transmission span by applying an active component (e.g. semiconductor laser) or highly nonlinear fiber (e.g. nonlinear phase-conjugating mirror). The short wavelengths of the signal are interchanged with the longer wavelengths making use of a nonlinearity based phase conjugation. This concept enables a full compensation of dispersion and dispersion

slope, but it is less practical for the implementation in the transmission systems because of its complexity.

Fiber Bragg Grating (FBG) modules are fabricated by implementing refractive index changes in the fiber core. The regions with different refractive indices are called gratings. Depending on the distance between the gratings known as grating period, which can be realized as constant or varying (chirped), the shorter wavelengths will be reflected before the longer ones. The consequence is pulse compression and dispersion compensation. FBGs represent a promising technology for the realization of dynamic dispersion compensation in tuneable dispersion compensators. The advantages of FBGs are large nonlinear tolerance and lower device loss.

Input pulse   Broadened pulse   Recompressed pulse

Optical fiber   FBG
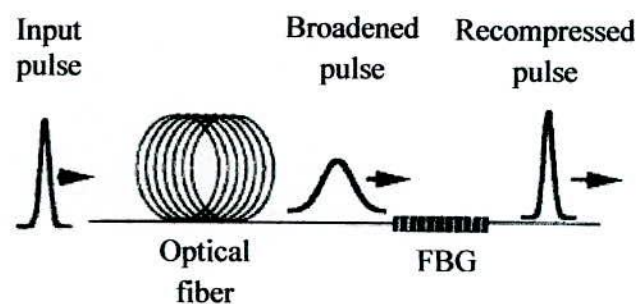
Fig. 2.11: Schematic illustration of a dispersion compensator designed for simultaneous compensation of GVD using fiber Bragg grating.

Among the compensation technique DCF gives good results but it is bulky, costly, and not easy to handle. On other hand FBG-based GVD compensator offers significant advantages such as ready integrability with all fiber optic systems, compactness and low fabrication cost [30-33]. In this study, a theoretical analysis is presented to investigate the BER performance of proposed model using FBG-based GVD compensator.

CHAPTER 3

Methodology

A theoretical analysis is presented to investigate the improvement of bit error rate (BER) performance of direct sequence optical code division multiple access with in-line optical amplifiers. In this analysis, intensity modulation direct detection technique is employed in single mode fiber operating at 1550nm, and optical orthogonal codes are used as address sequence. Optoelectronic conversion is performed by an avalanche photodiode in an optical correlator receiver. The system BER performance is determined in presence of GVD, PMD, and their compensators on account of receiver, optical amplifier, and multiuser access interference noises.

The aim of this chapter is to describe the proposed DS-OCDMA system and to also describe the mathematical model of the proposed system.

3.1 System Model
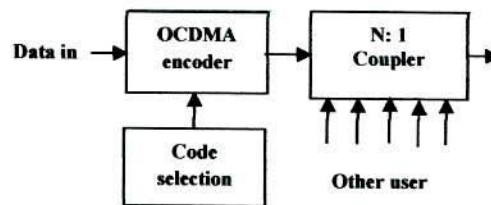
(a)
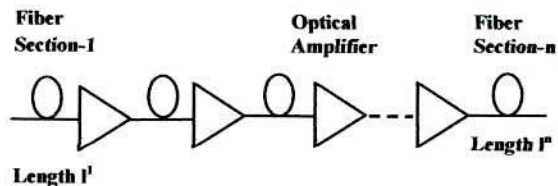
(b)
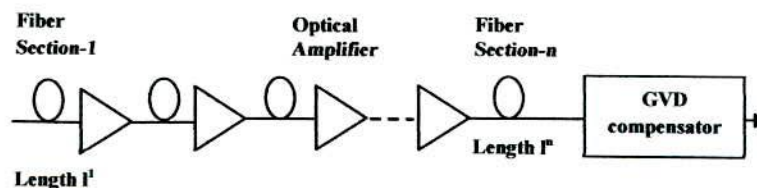
(c)
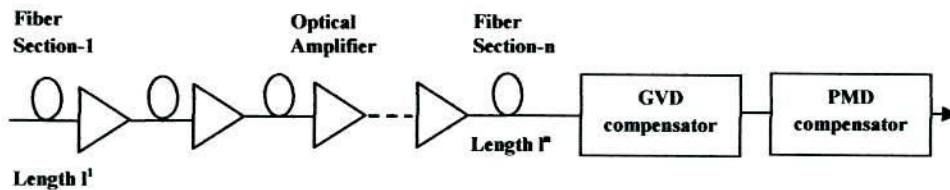
(d)
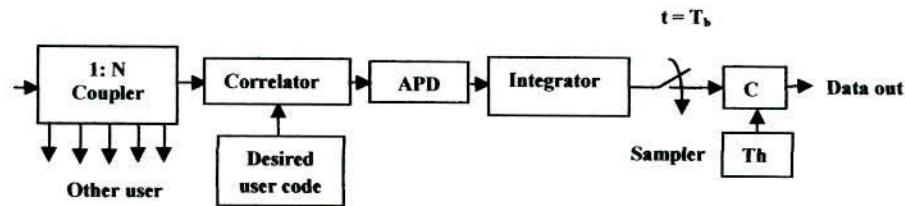
(e)

Fig. 3.1: Schematic block diagram of proposed OCDMA system (a) transmitter, (b) transmission medium, (c) transmission medium with GVD compensator, (d) transmission medium with GVD and PMD compensator, and (e) optical correlator receiver.

3.2 System Description

The schematic block diagram of an OCDMA transmitter, transmission medium, transmission medium with GVD compensator, transmission medium with PMD compensator, and optical correlator receiver is shown in Figs. 3.1 (a), (b), (c), (d), and (e), respectively. In the transmitter, a user's data is modulated by a unipolar signature sequence. The encoded signals of N number of users are coupled using an $N: 1$ coupler and transmitted through optical fiber transmission medium with n sections and $(n-1)$ in-line optical amplifiers. The gain of the amplifier is adjusted so that the loss of the optical signal in each fiber section is compensated. Erbium doped fiber amplifier (EDFA) is used as optical amplifier. In the receiver, a particular user data is recovered by the correlation operation between composite received signal and a replica of the desired user's address code that is carried out by an optical correlator receiver. The decoded signal is incident on the avalanche photodiode (APD). The output signal is integrated throughout the data bit period, and then compared with a threshold level at the comparator for data recovery. Fiber Bragg gating (FBG) based GVD compensator is used in the system to compensate the fiber optic GVD. We also consider another effect is called polarization mode dispersion (PMD) in fiber optic waveguide and a compensation technique used to compensate the PMD.

3.3 Theoretical Analysis

The mathematical model of the proposed DS-OCDMA is described in the following subsections:

3.3.1 GVD-Induced Pulse Broadening in Optical Fiber

We first consider of an initially transform-limited pulse of 1/e-width σ_0, broadened by propagation through optical fiber of length L with dispersion β_2^f. In this study, second-order fiber dispersion is considered. In case of super-Gaussian, the incident field can be written as [60]

$$g(0,t) = \exp\left[-\frac{1}{2}\cdot\left(\frac{t}{t_0}\right)^{2m}\right] \tag{3.1}$$

Where t_0 is the initial pulse width, and m is the order of super-Gaussian.

The super-Gaussian pulse is still keeps its shape for the super-Gaussian form in deliver process. After the distance of transmission L, the relation of the pulse width σ and initial pulse width $\sigma_0 = \left(t_0/\sqrt{2}\right)$ is given by [60]

$$\frac{\sigma}{\sigma_0} = \frac{1}{\sigma_b} = \left[1 + \frac{\Gamma(2-1/2m)}{\Gamma(3/2m)}\frac{\left(m\beta_2^f L\right)^2}{t_0^4}\right]^{1/2} \tag{3.2}$$

In case of Hyperbolic-Secant pulses, the incident field can be written as [60]

$$g(0,t) = \sec h\left(\frac{t}{t_0}\right) \tag{3.3}$$

The Hyperbolic-Secant pulse is still keeps its shape for the Hyperbolic-Secant form in deliver process. After the distance of transmission L, the relation of the pulse width σ and initial pulse width $\sigma_0 = (\pi/\sqrt{12})t_0$ is given by [60]

$$\frac{\sigma}{\sigma_0} = \frac{1}{\sigma_b} = \left[1 + \left(\frac{\pi\beta_2 L}{6\sigma_0^2}\right)^2\right]^{1/2} \tag{3.4}$$

3.3.2 Dispersion of Fiber Grating

The dispersion characteristics of an infinitely long grating are similar to those of a finite-length apodized grating. To a good approximation, the grating dispersion can be described by the following dispersion relation of a periodic structure, which is obtained using the coupled mode equations [30]

$$d^2 = \rho^2 + k^2 \tag{3.5}$$

where $d = (\omega - \omega_B)n/c$ is the detuning of the channel carrier frequency ω from the resonant Bragg frequency ω_B, and $\rho = \beta - \beta_B$ is the deviation of the propagation constant β from the Bragg wavenumber β_B, n is the mode index in a single-mode silica fiber, and c is the speed of light in vacuum. The coupling coefficient k is defined in the usual manner. The grating stop band is obtained corresponds to detuned frequencies $(|d| < k)$, where the reflectivity is high. At frequencies close to the stop band $(|d| > k)$, the grating exhibits strong second and higher-order dispersions, which strongly affect the light propagation. On the short-wavelength side of the stop band $(d > 0)$, the dispersion is anomalous. In contrast, on the long-wavelength side $(d < 0)$, the dispersion is normal and can be used for compensation of anomalous GVD of fibers in the 1550nm wavelength region. Clearly, at frequencies far from the stop band $(|d| \gg k)$ the grating plays no significant role, and the dispersion relation becomes identical to that of a uniform medium, i.e., $\rho \approx \pm d$. We only consider the second order dispersion β_2^g and third order dispersion β_3^g for fiber grating. The term $\beta_2^g(d)$ is the (quadratic) group velocity dispersion given by [30]

$$\beta_2^g(d) = -\left(\frac{n}{c}\right)^2 \frac{k^2}{(d^2 - k^2)^{3/2}} \times sign(d) \tag{3.6}$$

and $\beta_3^g(d)$ is the cubic dispersion which is given by [30]

$$\beta_3^g(d) = 3\left(\frac{n}{c}\right)^3 \frac{k^2 d}{(d^2 - k^2)^{5/2}} \tag{3.7}$$

Clearly, both β_2^g and β_3^g diverge at the band edge $(d = k)$.

In an ideal dispersion compensator, the dispersion of the grating is matched to that of the fiber, i.e.,

$$L_g \left| \beta_2^g \right| = L \left| \beta_2^f \right| \tag{3.8}$$

where β_2^g is the quadratic dispersion of the grating and β_2^f is the quadratic dispersion of the fiber. Here we define an ideal dispersion compensator to be that which recompresses the dispersion-broadened pulse to its transform-limited pulse width. Of course, the cubic dispersion of the grating acts to diminish the efficiency of compression and to distort the pulse, and thus must be as small as possible for the grating to approach ideal behavior.

3.3.3 Pulse Propagation in Fiber Bragg Grating

We now model the grating structure by a highly dispersive uniform medium with the quadratic dispersion β_2^g and cubic dispersion β_3^g. This allows us to use the wave equation instead of solving coupled-mode equations to study pulse propagation in the grating. As we neglect fourth and higher order dispersion, the slowly varying amplitude of the pulse envelope satisfies

$$\left(\frac{\partial}{\partial z} + \frac{i \beta_2^g}{2} \frac{\partial^2}{\partial t^2} - \frac{\beta_3^g}{6} \frac{\partial^3}{\partial t^3} \right) g(z,t) = 0 \tag{3.9}$$

where z is the axial position along the grating. When a GVD-broadened pulse width σ_1 propagates through the grating then pulse width is recompressed to σ_2. The rms pulse width after propagating in a grating of length L_g can be found analytically for the case including quadratic and cubic dispersion. The ratio of initial pulse width σ_0 and recompressed pulse width σ_2, can be written as [31]

$$\frac{\sigma_0}{\sigma_2} = \sigma_b = \frac{\sigma_0}{\sigma_1} \left[\left(1 + \beta_2^g L_g \alpha_f \right)^2 + \left(\frac{L_g \beta_2^g}{2\sigma_1^2} \right)^2 + \left[1 + (2\alpha_f \sigma_1^2)^2 \right] \frac{1}{8} \left(\frac{L_g \beta_3^g}{2\sigma_1^3} \right)^2 \right]^{-1/2} \tag{3.10}$$

Where the chirp parameter (α_f) of Gaussian pulse is given by [30]

$$\alpha_f = \frac{L}{\beta_2^f\left[L^2 + \left(\frac{2\sigma_0^2}{\beta_2^f}\right)^2\right]} \tag{3.11}$$

3.3.4 Pulse broadening due to PMD

The rms pulse width broadened due to the PMD is given by [61]

$$\sigma^2 = \sigma_0^2 + \frac{1}{4}\left[\langle\Omega^2\rangle - (s.\langle\Omega\rangle)^2\right] \tag{3.12}$$

where Ω and s are the input PMD vector and the input state of polarization (SOP), respectively, σ_0 is the initial rms pulse width defined as $\sigma_0^2 = (1/2\pi)\int_{-\infty}^{\infty}t^2|f(t)|^2dt$, and the

bracket denotes frequency average such that $\langle a\rangle = \int_{-\infty}^{\infty}a|f(w)|^2dw$. $f(t)$ and $f(w)$ are the initial pulse amplitude and its Fourier transform, respectively. It should be noted that (3.12) includes all higher order PMD effects and does not depend on the pulse shape. If we define an expected rms broadening $b\left(=\frac{1}{\sigma_b}\right)$ as

$$b^2 = E\left\{\frac{\sigma^2}{\sigma_0^2}\right\} = 1 + \frac{1}{4\sigma_0^2}\left[E\{\langle\Omega^2\rangle\} - E\{s.\langle\Omega\rangle)^2\}\right] \tag{3.13}$$

where $E\{.\}$ denotes expectation value. From (3.13), the broadening factor due to the PMD is given by [61, 62]

$$b_{UC}^2 = 1 + \frac{1}{4\sigma_0^2}\left[E\{\Delta\sigma^2\} - \frac{1}{3}\int_{-\infty}^{\infty}\int_{-\infty}^{\infty}G(w_1-w_2).\frac{|f(w_1)|^2|f(w_2)|^2}{4\pi^2}dw_1dw_2\right] \tag{3.14}$$

where $\Delta\sigma$ is the magnitude of the PMD vector $\left(=|\Omega|\right)$, referred to as the differential group delay (DGD). In deriving (3.14), the order of the frequency integration and averaging was changed, and the frequency correlation of the PMD vector is used, which is given by [63]

$$E\{\Omega_i(w_1)\Omega_j(w_2)\}=\frac{1}{3}\delta(i-1)G(w_1-w_2)=\delta(i-1)\frac{1-\exp\left[-\dfrac{E\{\Delta\sigma^2\}}{3}(w_1-w_2)^2\right]}{(w_1-w_2)^2}. \quad (3.15)$$

For an *intensity normalized Gaussian initial pulse*, the broadening factor is calculated analytically and given by

$$b_{UC}^2=1+z-\frac{1}{2}\left[\left(1+\frac{4z}{3}\right)^{\frac{1}{2}}-1\right] \quad (3.16)$$

where

$$z=\frac{E\{\Delta\sigma^2\}}{4\sigma_0^2}=\frac{D_{PMD}^2 L}{4\sigma_0^2}. \quad (3.17)$$

Here L is the length of the fiber, and D_{PMD} is the polarization mode dispersion coefficient. The frequency correlations between the higher order PMD vectors, which are defined as frequency derivatives of the PMD vector, can be derived by differentiating (3.15)

$$E\{\Omega^{(u)}(w_1).\Omega^{(v)}(w_2)\}=\frac{d^{(u+v)}G}{dw_1^u dw_2^v} \quad (3.18)$$

which also gives us the expectation of the higher order PMD vector as a function of $E\{\Delta\sigma^2\}$. In (3.18), $\Omega^{(v)}$ is the vth-frequency derivative of the PMD vector, that is, the $(v+1)th$-order PMD vector.

3.3.5 PMD Compensation with frequency advanced higher-order PMD vectors

In this section, a simple approach to higher-order PMD compensation is presented with frequency advanced higher-order PMD vectors. The idea is to use the frequency average of the higher order PMD vector of the fiber in emulating the compensation PMD vector. The compensation PMD vector will be in the form of $\Omega_c=\langle\Omega\rangle+\langle\Omega^{(1)}\rangle w+\langle\Omega^{(2)}\rangle(w^2/2)....$.

This compensation vector may not be a good approximation of the fiber PMD vector near

the center frequency for large PMD values, but in terms of PMD compensation, it may be more effective. The performance of this approach is also analyzed in the chapter 4.

A. First-Order Compensation

In the first-order compensation, the total PMD vector is $\Omega_{1st} = \Omega - \langle \Omega \rangle$, and the broadening factor is calculated in the same way

$$E\left\{\langle \Omega_{1st}^2 \rangle\right\} = E\left\{\langle \Omega^2 \rangle\right\} - E\left\{\langle \Omega \rangle^2 \right\}$$

$$= E\{\Delta\sigma^2\} - \int_{-\infty}^{\infty} \int_{-\infty}^{\infty} G(w_1 - w_2) \cdot \frac{|f(w_1)|^2 |f(w_2)|^2}{4\pi^2} dw_1 dw_2 \qquad (3.19)$$

$$b_{1st}^2 = 1 + z - \frac{3}{2}\left[\left(1 + \frac{4z}{3}\right)^{1/2} - 1\right]. \qquad (3.20)$$

B. Second-Order Compensation

Applying the idea to the second-order compensation, the total PMD vector becomes $\Omega_{2nd} = \Omega - \langle \Omega \rangle - \langle \Omega^{(1)} \rangle w$ and the broadening factor is obtained as follows:

$$E\left\{\langle \Omega_{2nd}^2 \rangle\right\} = E\left\{\langle \Omega_{1st}^2 \rangle\right\} + E\left\{\langle \Omega^{(1)} \rangle^2 \langle w^2 \rangle - 2\langle \Omega \langle \Omega^{(1)} \rangle w \rangle\right\}$$

$$= E\left\{\langle \Omega_{1st}^2 \rangle\right\} + \langle w^2 \rangle \int_{-\infty}^{\infty} \int_{-\infty}^{\infty} \frac{d^2 G}{dw_1 dw_2} \cdot \frac{|f(w_1)|^2 |f(w_2)|^2}{4\pi^2} dw_1 dw_2$$

$$- 2\int_{-\infty}^{\infty} \int_{-\infty}^{\infty} \frac{dG}{dw_2} w_1 \frac{|f(w_1)|^2 |f(w_2)|^2}{4\pi^2} dw_1 dw_2 \qquad (3.21)$$

$$b_{2nd}^2 = b_{1st}^2 + \frac{3}{2}\left(1 + \frac{4z}{3}\right)^{3/2} - 3(z+1)\left(1 + \frac{4z}{3}\right)^{1/2} + \left(\frac{4z^2}{3} + 2z\right)\left(1 + \frac{4z}{3}\right)^{-1/2} + \frac{3}{2} \qquad (3.22)$$

C. Third-Order Compensation

In the third-order compensation, the total PMD vector is $\Omega_{3rd} = \Omega - \langle \Omega \rangle - \langle \Omega^{(1)} \rangle w - \langle \Omega^{(2)} \rangle (w^2/2)$, and the broadening factor is calculated as follows:

$$E\left\{\left\langle\Omega_{3rd}^2\right\rangle\right\} = E\left\{\left\langle\Omega_{2nd}^2\right\rangle\right\} + E\left\{\left\langle\Omega^{(2)}\right\rangle^2\left\langle\frac{w^4}{4}\right\rangle - \left\langle\Omega.\left\langle\Omega^{(2)}\right\rangle w^2\right\rangle + \left\langle\Omega\right\rangle.\left\langle\Omega^{(2)}\right\rangle\left\langle w^2\right\rangle\right\}$$

$$= E\left\{\left\langle\Omega_{2nd}^2\right\rangle\right\} + \frac{1}{4}\left\langle w^4\right\rangle\int_{-\infty}^{\infty}\int_{-\infty}^{\infty}\frac{d^4G}{dw_1^2 dw_2^2}\frac{\left|f(w_1)\right|^2\left|f(w_2)\right|^2}{4\pi^2}dw_1 dw_2$$

$$-\int_{-\infty}^{\infty}\int_{-\infty}^{\infty}\frac{d^2G}{dw_2^2}w_1^2\frac{\left|f(w_1)\right|^2\left|f(w_2)\right|^2}{4\pi^2}dw_1 dw_2 + \left\langle w^2\right\rangle\int_{-\infty}^{\infty}\int_{-\infty}^{\infty}\frac{d^2G}{dw_2^2}\frac{\left|f(w_1)\right|^2\left|f(w_2)\right|^2}{4\pi^2}dw_1 dw_2$$

$$(3.23)$$

$$E\left\{\left(s.\left\langle\Omega_{3rd}\right\rangle\right)^2\right\} = E\left\{\left(s.\left(-\left\langle\Omega^{(2)}\right\rangle\left\langle\frac{w^2}{2}\right\rangle\right)\right)^2\right\}$$

$$= \frac{\left\langle w^2\right\rangle^2}{12}\int_{-\infty}^{\infty}\int_{-\infty}^{\infty}\frac{d^4G}{d^2w_1 d^2w_2}\frac{\left|f(w_1)\right|^2\left|f(w_2)\right|^2}{4\pi^2}dw_1 dw_2 \qquad (3.24)$$

$$b_{3rd}^2 = b_{2nd}^2 + 2\left(1+\frac{4z}{3}\right)^{5/2} - \left(\frac{20z}{3}+\frac{3}{4}\right)\left(1+\frac{4z}{3}\right)^{3/2} + \left(\frac{20z^2}{3}+\frac{3z}{2}-\frac{9}{4}\right)\left(1+\frac{4z}{3}\right)^{1/2}$$

$$-\left(\frac{32z^3}{27}+\frac{2z^2}{3}-\frac{3}{2}z\right)\left(1+\frac{4z}{3}\right)^{-1/2} - \left(\frac{64z^4}{81}-\frac{2z^2}{3}\right)\left(1+\frac{4z}{3}\right)^{-3/2} + 1 \qquad (3.25)$$

3.3.6 The BER Calculation

In this analysis, the effects of shot noise, surface leakage current and thermal noise current associated with APD receiver are considered. Furthermore, we assume that all users have the same effective power at any receiver, the identical bit rate and signal format. For an OCDMA system with N transmitter and receiver pairs (users), the received signal $y_{out}(t)$ is the sum of N user's transmitted signals, which can be given by

$$y_{out}(t) = P_R \sum_{i=1}^{N}\sum_{j=1}^{F} B_i A_i(j)\int_{\alpha_i+jT_c}^{\alpha_i+(j+1)T_c} g(t-\alpha_i-jT_c)dt \qquad (3.26)$$

where P_R is the received pulse peak power, B_i is the i-th user's binary data bit (either "1" or "0") with duration T_b at time t ($0 < t \leq T_b$), $A_i(j)$ is the j-th chip value (either "1" or

"0") of the i-th user address code with code length $y_{out}(t)$, code weight W, and α_i is the time delay associated with the i-th user's signal. Without loss of generality, we assume that user 1 is the desired user, all delays α_i at the receiver are relative to the first user delay only, i. e., $\alpha_1 = 0$. $g(t)$ is the Gaussian function with period T_c, and satisfies the normalization condition. All users are assumed chip synchronous, i.e., $\alpha_i = nT_c$, and $0 \le n < F$ is an integer. In that case, the multiple access interference (MAI) will be maximum and the BER will be an upper bound on the BER for the chip asynchronous case. At the receiving terminal, the correlation operation between signal $y_{out}(t)$ and a replica of the desired user's address code is carried out by an optical correlator receiver to achieve decoding. The decoding signal is incident on the APD. Output photocurrent Y_1 sampled at time $t = T_b$ can be written as

$$Y_1 = \mu' + \mu'' + \mu_n + \mu_A \tag{3.27}$$

Where μ' is the desired user's signal current, μ'' the interference signal current due to MAI, μ_n the APD noise currents which includes shot noise current, bulk dark current, surface leakage current, and thermal noise current, and μ_A optical amplifier noise currents (i.e. signal-spontaneous beat noise, spontaneous-spontaneous beat noise). We assume that the $(F, W, g(t))$ OOC's selected as user address codes. By the correlation definition of OOC's, each interference user can contribute at most one hit during the correlation time. If γ denotes the total number of hits from interference users, the probability density function of γ is given by

$$P(\gamma) = \binom{N-1}{\gamma} p^\gamma q^{N-1-\gamma} \tag{3.28}$$

Where $p = W^2/2F$, $q = 1 - p$ and γ is an integer ($0 \le \gamma \le N-1$). If code length F, code weight W and γ are given, the first two terms in (3.27) can be determined. We assume that the APD noise current has Gaussian nature. The output photocurrent Y_1 can be regarded as a Gaussian random variable. Its average I_1 and variance τ_1^2 for bit "1" and "0". Since the received signal is multiplied by the user address code, i.e., (0,1) sequence. During the bit "1" interval of the desired signal, photons fall on the APD only during the

W mark intervals and are totally blocked during the $F-W$ space intervals. During the W chip intervals of the desired signal, the total number of pulses (either marks or spaces) due to N users is WN. Among these WN pulses, there are $W+\gamma$ mark pulses with power level $\sigma_b P_R$, and $WN-(W+\gamma)$ space pulses with power level $\sigma_b \varepsilon P_R$. Here, σ_b include the effect of the fiber impairments, and ε is the extinction ratio of APD receiver. Therefore, for data bit "1" the average photocurrent I_1 and noise variance τ_1^2 are given by

$$I_1 = M\left(R_0 G P_t^1 + I_{BD}\right) + I_{SL} \tag{3.29}$$

$$\tau_1^2 = 2eM^{2+x}\left(R_0 G P_t^1 + I_{BD}\right)B_e + 2eI_{SL}B_e + \frac{4\kappa_B T}{R_L}$$
$$+ \frac{4GI_S^1 I_{SP} L^2 B_e}{B_0} + \frac{(I_{SP}L)^2 B_e (2B_0 - B_e)}{B_0^2} \tag{3.30}$$

where the exponent x varies between 0 and 1.0 depending on the APD material and structure, M the average APD gain, R_0 the unity gain responsivity, e an electron charge, I_{BD} the average bulk dark current, which is multiplied by the avalanche gain, I_{SL} the average surface leakage current, which is not affected by avalanche gain, B_e the receiver electrical bandwidth, κ_B the Boltzmann's constant, T the receiver noise temperature, and R_L the receiver load resistor.

$$P_t^1 = (W+\gamma)\sigma_b P_R + (WN-W-\gamma)\sigma_b \varepsilon P_R \tag{3.31}$$

$$I_{SP} = N_A N_{SP}(G-1)eB_0 \tag{3.32}$$

$$I_S^1 = \frac{2e\varepsilon P_R}{h\nu(\varepsilon+1)} \tag{3.33}$$

where N_{SP} is the spontaneous emission factor, N_A is the number of optical amplifier, G is the gain of optical amplifier. σ_b is the ratio of initial rms pulse width σ_0 to output rms pulse width σ.

For data bit "0", the average photocurrent I_0 and noise variance τ_0^2 of Y_1 can be determined in the same way as for data bit "1". In this case, I_0 and τ_0^2 can be written as

$$I_0 = M(R_0 GP_t^0 + I_{BD}) + I_{SL} \tag{3.34}$$

$$\tau_0^2 = 2eM^{2+x}(R_0 GP_t^0 + I_{BD})B_e + 2eI_{SL}B_e + \frac{4\kappa_B T}{R_L}B_e$$
$$+ \frac{4GI_S^0 I_{SP}L^2 B_e}{B_0} + \frac{(I_{SP}L)^2 B_e(2B_0 - B_e)}{B_0^2} \tag{3.35}$$

where

$$P_t^0 = \gamma\sigma_b P_R + (WN - \gamma)\sigma_b \varepsilon P_R \tag{3.36}$$

$$I_S^0 = \frac{2eP_R}{h\nu(\varepsilon + 1)} \tag{3.37}$$

For the desired user's data bit "1" or "0", the conditional probability density function of the output photocurrent Y_1 can be expressed as

$$P_{Y_1}(I|\gamma,1) = \frac{1}{\sqrt{2\pi\tau_1^2}} \exp\left[\frac{-(I - I_1)^2}{2\tau_1^2}\right] \tag{3.38}$$

$$P_{Y_1}(I|\gamma,0) = \frac{1}{\sqrt{2\pi\tau_0^2}} \exp\left[\frac{-(I - I_0)^2}{2\tau_0^2}\right] \tag{3.39}$$

For a given threshold level I_D, the probability of errors for bit "1" and "0" are calculated by

$$P_e^{(1)}(\gamma) = \int_0^{I_D} P_{Y_1}(I|\gamma,1)dI = \frac{1}{2}erfc\left(\frac{I_1 - I_D}{\sqrt{2\tau_1^2}}\right) \tag{3.40}$$

$$P_e^{(0)}(\gamma) = \int_{I_D}^{\infty} P_{Y_1}(I|\gamma,0)dI = \frac{1}{2}erfc\left(\frac{I_D - I_0}{\sqrt{2\tau_0^2}}\right) \tag{3.41}$$

The probability of error per bit, depended on the threshold level I_D, is defined as

$$P_e(\gamma) = \frac{1}{2}\left[P_e^{(1)}(\gamma) + P_e^{(0)}(\gamma)\right] \tag{3.42}$$

The threshold level I_D, is defined as

$$I_D = \frac{\tau_0 I_1 + \tau_1 I_0}{\tau_0 + \tau_1}$$

(3.43)

Here, we assume that the bit "1" and "0" have the identical probability. The total probability of error P_e per bit is given by

$$P_e = \sum_{\gamma=0}^{N-1} P_e(\gamma) \binom{N-1}{\gamma} p^\gamma q^{N-1-\gamma}$$

(3.44)

CHAPTER 4

Results and Discussion

Using the mathematical formulations presented in Chapter 3, the BER performance of DS-OCDMA system is evaluated in the dispersive fiber medium. The purpose of this chapter is to present the numerical results obtained for the proposed OCDMA system. In Section 4.1 the impact of GVD on the BER performance of proposed system is presented. The chipshape-dependent performance of the proposed OCDMA system in presence of GVD is discussed in Section 4.2. Section 4.3 presents the improvement of BER performance of proposed system using FBG-based GVD compensator. Influence of PMD on the BER performance of the proposed system is described in Section 4.4. Also, performance improvement of the proposed system is presented in Section 4.5 in presence of PMD compensation using frequency advanced higher-order PMD vectors.

4.1 Performance Analysis in Presence of GVD

Following the analytical formulations presented in Chapter 3, the BER performance of a DS-OCDMA system is evaluated including the effect of GVD. In the numerical calculations, Gaussian shaped OOC's are used as user address sequence. For optoelectronic conversion InGaAs-based APD is used in the system receiver. Its primary parameters are taken as follows: mean gain $M = 20$, Excess noise index $x = 0.7$, bulk dark current $I_{BD} = 2$ nA, and surface leakage current $I_{SL} = 10$ nA. Other parameters are receiver load resistor $R_L = 1000$ Ω, and extinction ratio $\varepsilon = 0.05$. The parameters of the single mode fiber used for numerical computations are: chromatic dispersion co-efficient D = 18 ps/(km.nm) for wavelength $\lambda = 1550$ nm and fiber attenuation = 0.2dB/km.

Figure 4.1 depicts the plot of BER versus number of simultaneous users. The results are obtained for Gaussian-shaped chip as a function of chip rates when fiber length= 50km. It is found that the BER performance of the proposed system is strongly dependent on the number of simultaneous users, and chip rates. The BER performance degrades with large number of users due to the effect of MAI for all values of chip rate. It is also found that the BER performance is aggravated with increasing chip rates due to interchip interference caused by dispersion-induced broadening. The possibility of interchip interference

increases with increasing chip rate, because of shortest chip duration even for the small fiber length.

Figure 4.2 shows the BER versus number of simultaneous user curves plotted as a function of fiber lengths at constant 10Gchip/s. It is found that the BER increase with increase in fiber length from 50km to 200km. It can be interred that, with increasing transmission distance the dispersion-induced pulse broadening becomes severe. As a result, the proposed system BER performance degraded more with increasing fiber length.

Figure 4.3 shows the plot of BER versus received signal power with variable chip rates; and constant fiber length of 200km and number of simultaneous users 10. It is found that higher received signal power is needed when chip rate changes from 10Gchip/s to 20Gchip/s in order to maintain a BER of 10^{-9}. This is due to dispersion-induced pulse shape distortion which increases with increasing chip rate. For a particular value of chip rate, SNR increases with increasing received signal power, and hence the system BER performance is found to improve.
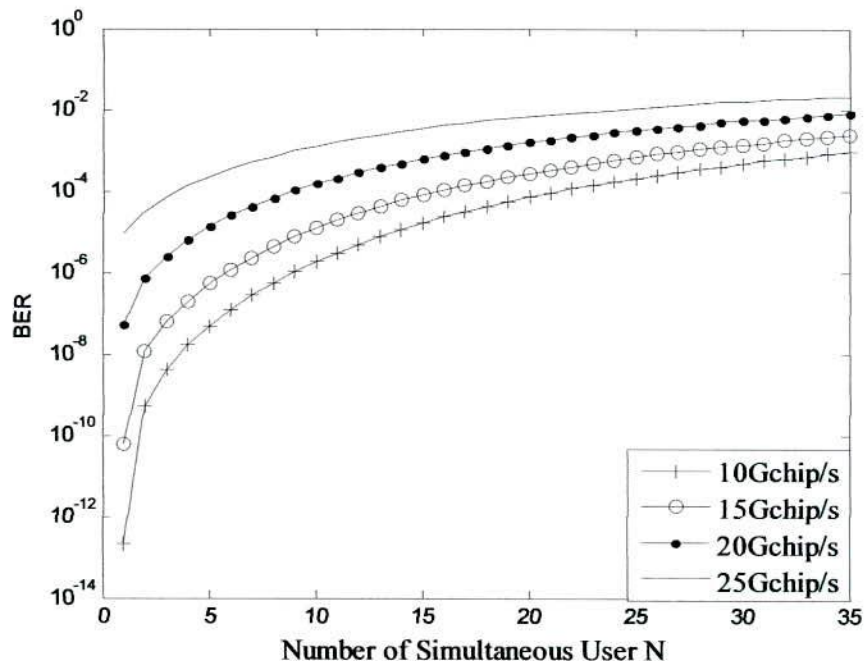

Fig. 4.1: Plot of BER versus number of simultaneous users with variable chip rates and constant fiber length of 50km.
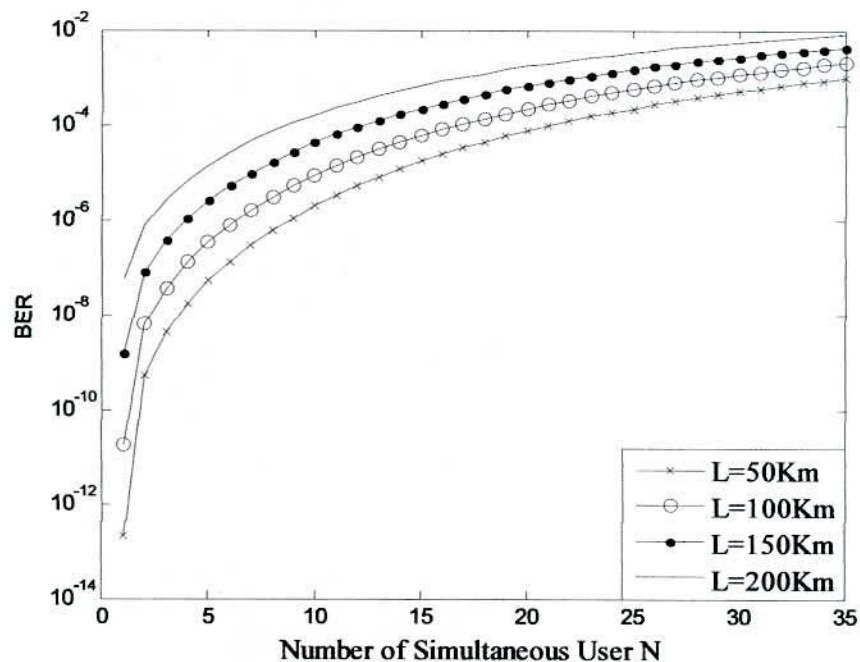
Fig. 4.2: Plot of BER versus number of simultaneous users with different fiber lengths when chip rate =10Gchip/s.
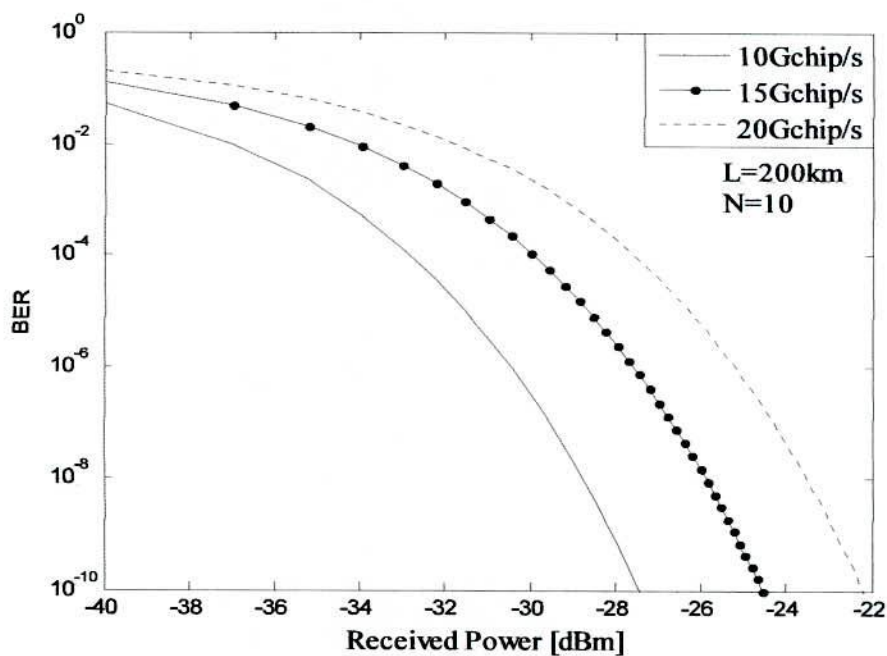

Fig. 4.3: Plot of BER versus received power with different chip rate when fiber length = 200km and number of simultaneous users =10.
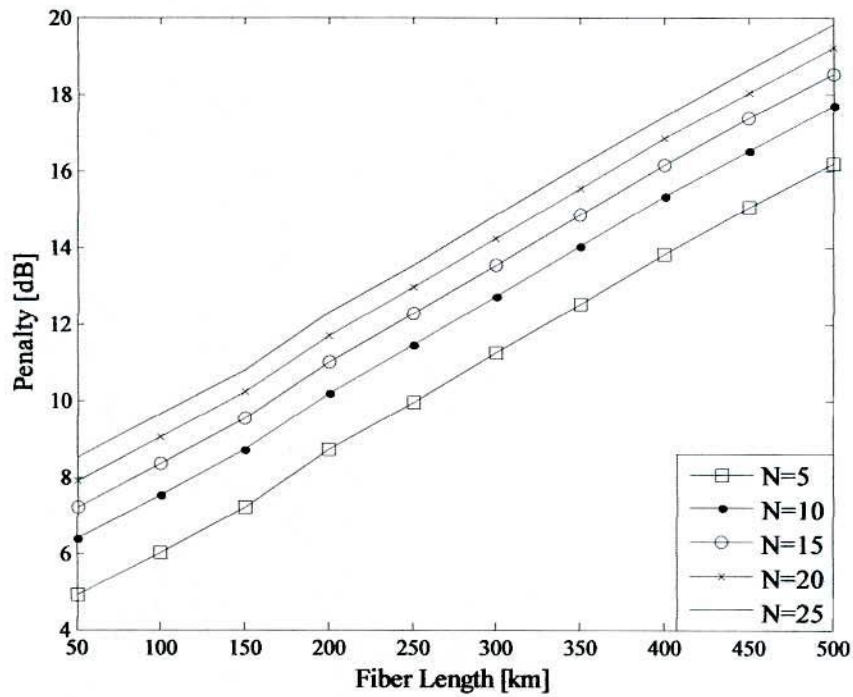
Fig. 4.4: Plot of power penalty versus fiber length for different number of simultaneous users when chip rate = 10Gchip/s.
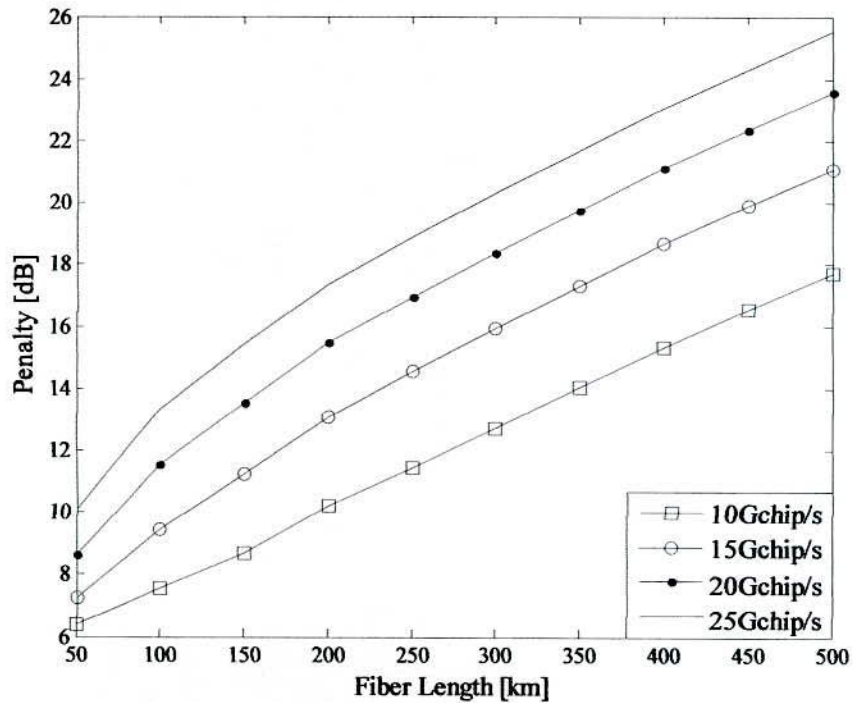

Fig. 4.5: Plot of power penalty versus fiber length for different chip rates when number of simultaneous users 10.

The power penalty suffered by the system is determined at BER of 10^{-9} and plotted in Fig. 4.4 with respect to fiber length for different number of simultaneous users in presence of GVD at chip rate 10Gchip/s. It is found that power penalty for the proposed system increases with increasing fiber length. This is because GVD-induced pulse broadening increases with fiber length resulting in degradation of the system SNR. The typical values of power penalty are 6.4 dB and 12.73 dB for fiber length 50km and 300km at 10Gchip/s and number of simultaneous user 10. It is also found that the power penalty increases with increasing number of simultaneous user due to the effect of MAI.

Figure 4.5 depicts the plot of power penalty versus fiber length for different chip rates. The results are obtained in presence of GVD for the number of simultaneous users 10. It is observed in Fig. 4.5 that the power penalty increased with increasing the fiber length due to the fiber optic dispersion. It is also found that the system performance severely degrades with increasing chip rate due to interchip interference caused by GVD-induced spreading and overlapping of short duration chips.

From above results it is cleared that the numbers of simultaneous users are limited by the MAI-induced effect in DS-OCDMA system. It is also found that GVD-induced effect severely degrades the system performance which also limits the maximum transmission fiber length and higher chip rate.

In this section, the BER performance of the proposed OCDMA system is discussed for the Gaussian-shaped chips. Since the system power penalty severely degrades with chip rates it is very much important to study the system performance further with chip shape. In order to do so, super Gaussian and Hyperbolic-Secant chip shapes are chosen and the details are discussed in the next section.

4.2 Chipshape-dependent Performance in Presence of GVD

In previous studies [22, 23], performance of OCDMA is investigated using rectangular-shaped OOC's. It is well know that rectangular shaped waveform contains more harmonics that may lead to overlapping of chips due to GVD of fiber optic waveguide. It is anticipated that GVD-induced pulse shape broadening can be reduced using Gaussian or other chipshapes containing less harmonics. To understand the chipshape-dependent performance of OCDMA, super Gaussian shaped chips are used that can be converted from Gaussian to rectangular shaped depending on the order of super Gaussian. Further the

performance of super Gaussian-shaped chips is compared with an advanced chipshaped called Hyperbolic-Secant. Using the analytical formulations in the previous chapter 3, the Chipshape-dependent BER performance of DS-OCDMA is analytically studied.

The power penalty suffered by the system is determined at BER of 10^{-9} and plotted in Fig. 4.6 with respect to the number of simultaneous users for Hyperbolic-Secant shaped chip and different order of super-Gaussian shaped chip in presence of GVD. The results are obtained at chip rate 10Gchip/s, and fiber length=200km. It is found that power penalty *increases with increasing number of simultaneous users due to the combined effects of MAI, and GVD.* It is also found that the system suffers more penalty with increasing the order of super-Gaussian (m). This is because super-Gaussian shaped chip become rectangular-shaped chip, with the increasing the value of m, which contains more harmonics. However, the power penalties are reduced by 1.15dB for N =10 and 0.9dB for N =15 when Hyperbolic-Secant shaped chip is considered instead of 1st order super-Gaussian shaped chip. The same results are found to be 4.45dB and 4.2dB in case of 4th order super-Gaussian shaped chip.
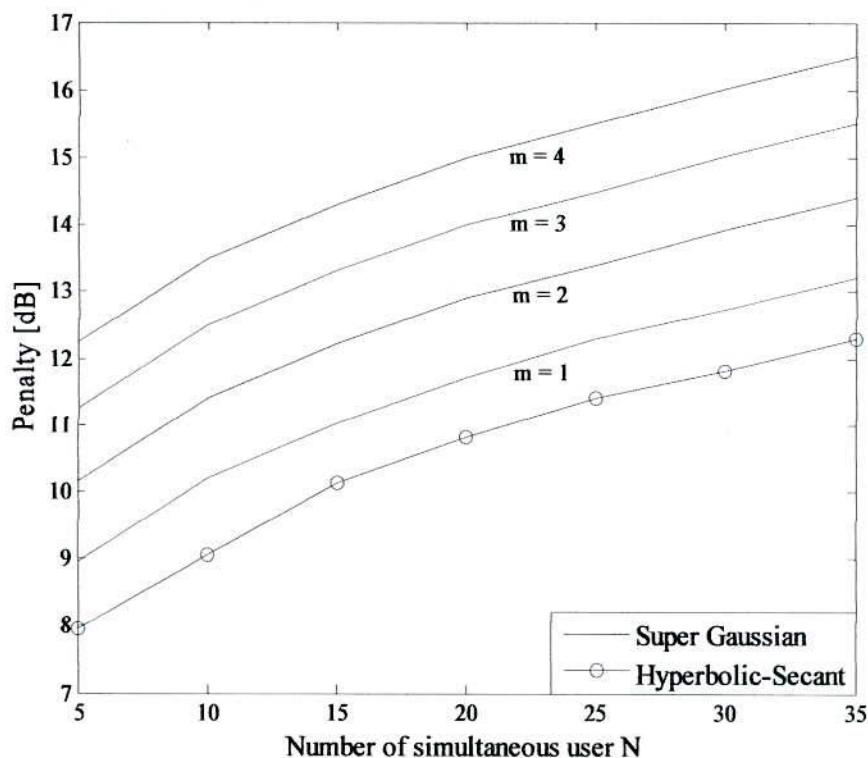

Fig. 4.6: Plot of power penalty versus number of simultaneous user for Super-Gaussian and Hyperbolic-Secant shaped chip in presence of GVD at chip rate 10Gchip/s, and fiber length of 200km.
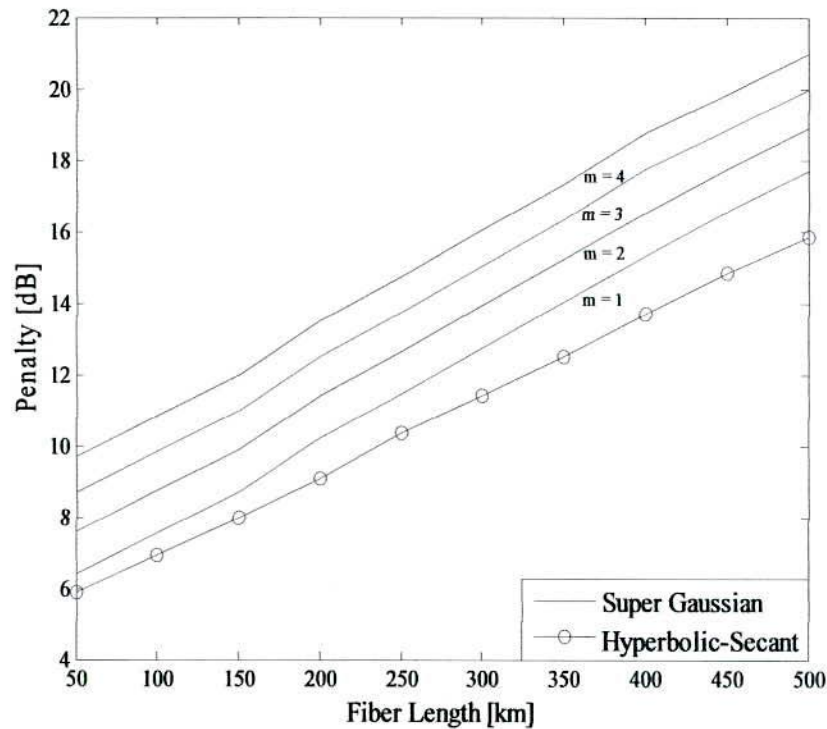
Fig. 4.7: Plot of power penalty versus fiber length for Super-Gaussian and Hyperbolic-Secant shaped chip in presence of GVD at chip rate 10Gchip/s, and number of simultaneous user 10.

It is also observed in Fig. 4.7 that the power penalty increases with increasing fiber length due to the dispersion. In case of Hyperbolic-Secant shaped chip the power penalty reduced by 0.5dB and 1.15dB respectively, for 50km and 200km fiber length with respect to 1st order super-Gaussian shaped chip when number of user is $N =10$. The dispersion-induced penalty found to increase significantly with increasing order of super-Gaussian. The chipshape-dependent performance is presented in this section demonstrates that the power penalty suffered by the OCDMA system can be reduced using Hyperbolic-Secant shaped address sequence. However, still due to dispersion-induced power penalty, long distance communication will be limited in OCDMA system. It is therefore very much important to employ suitable dispersion management technique for improving performance of the OCDMA system proposed here.

4.3 Performance Improvement using FBG-Based GVD Compensator

There are many approaches for managing GVD in fiber optic communication as discussed in previous chapter. Among the dispersion management techniques FBG-based GVD compensator is more compact, can be integrated easily with fiber optic system, and gives better performance. Using the mathematical formulations presented in previous chapter 3, the BER performance for the proposed OCDMA system is evaluated in presence of FBG-based GVD compensator. The GVD parameter of a SMF operating at 1550 nm is taken as 18 ps/(km.nm). In this analysis, Gaussian shaped OOCs are used as user address sequence and number of user =1.

Figure 4.8 shows BER versus received power plotted for the variation of fiber Bragg grating length from 0-14cm while the fiber length, chip rate, detuning, and coupling strength are fixed at 50km, 40Gchip/s, -8cm^{-1}, and 4cm^{-1}, respectively. It is found that the receiver sensitivity improves with increasing grating length. There is an optimum grating length (OGL) for which the system BER is found minimum. If the grating length is increased above the OGL the system BER performance starts degrading. This is because the group delay induced due to dispersion for a particular fiber length can be compensated by FBG-based compensator with OGL. After the OGL, instead of compensation, the pulse width starts broaden with increasing grating length according to (3.8) and (3.10).

The power penalty suffered by the system is determined at BER of 10^{-9} and plotted in Figs. 4.9-4.11 as a function of fiber length with the variation of grating length, coupling strength, and detuning, respectively. The results are estimated at chip rate of 40Gchip/s. As seen in Fig. 4.9 the dispersion-induced penalty compensates rapidly with grating length to a point where optimum compensation is obtained. After the optimum compensation the dispersion-induced penalty increases sharply with grating length. It is also found that the OGL, for which the optimum compensation is obtained, strongly depends on the fiber length. The stimulated grating lengths are found to be 9.5cm, 14cm, 19cm, and 24cm for the fiber lengths of 50km, 75km, 100km, and 125km, respectively. This is because the fiber optic GVD increases with fiber length. To compensate GVD-induced pulse broadening that occurs from longer fiber length, longer grating length is required. It is also found in Fig. 4.9 that there is a constant penalty (1.24dB) called threshold penalty that can not be compensated with the variation of grating length. This may be degradation of

grating performance due to third order dispersion. Similar results are found in Fig. 4.10 and Fig. 4.11 when the grating parameters such as coupling strength and detuning are varied. The optimum coupling strength is found 3.9cm^{-1}, 4.46cm^{-1}, 4.84cm^{-1}, and 5.13cm^{-1} for the fiber length 50km, 75km, 100km, and 125km, respectively. In Fig. 4.10 it is observed that the threshold penalty is not constant with fiber length rather it increases with coupling strength. When fiber length is 50km, the threshold penalty is evaluated to be 1.198dB. However, the threshold penalty is evaluated to be 1.793dB when fiber length is increased to 125km. This is may be degradation of grating performance due to direct correlation of coupling strength and third order grating dispersion as shown in (3.7). Similar results are also found in Fig. 4.11 where optimum values of detuning are evaluated -8.15cm^{-1}, -7.37cm^{-1}, -6.89cm^{-1}, and -6.56cm^{-1} for the fiber lengths of 50km, 75km, 100km, and 125km, respectively. Here the threshold penalty found to increase more with fiber length. The typical values are evaluated to be 1.172dB and 2.134dB for the fiber lengths of 50km and 125km, respectively. This is may be due to the fact that the third-order gating dispersion increases more with increasing the values of detuning according to (3.7).

It is also shown in Fig. 4.12-4.13 that the OGL for a particular fiber length highly depends on the detuning and coupling strength. It is found from Fig. 4.12 that the OGL increases with increasing detuning. This is because the inverse relationships between second-order gating dispersion and detuning. It is found from Fig. 4.13 that the OGL decrease with increasing coupling strength. This may due to the fact that the second-order gating dispersion is directly proportional to coupling strength.

To understand the performance of FBG-based compensator as a function of chip rate the power penalty suffered by the system is determined at BER of 10^{-9}. The results are shown in Fig. 4.14. It is found that the GVD-induced penalty is almost negligible below 10Gchip/s and increases sharply when chip rate increases above 10Gchip/s. This is because inter chip interference increases with increasing chip rate due to dispersion. The GVD-induced penalty is compensated using FBG-based compensator. The results are also shown in Fig. 4.14 in which the GVD-induced penalty is compensated about 85%, 80%, and 78% at chip rate of 40Gchip/s, 60Gchip/s, and 80Gchip/s, respectively. This is because FBG-based compensator can not be used for full compensation due to third-order dispersive effects in grating.
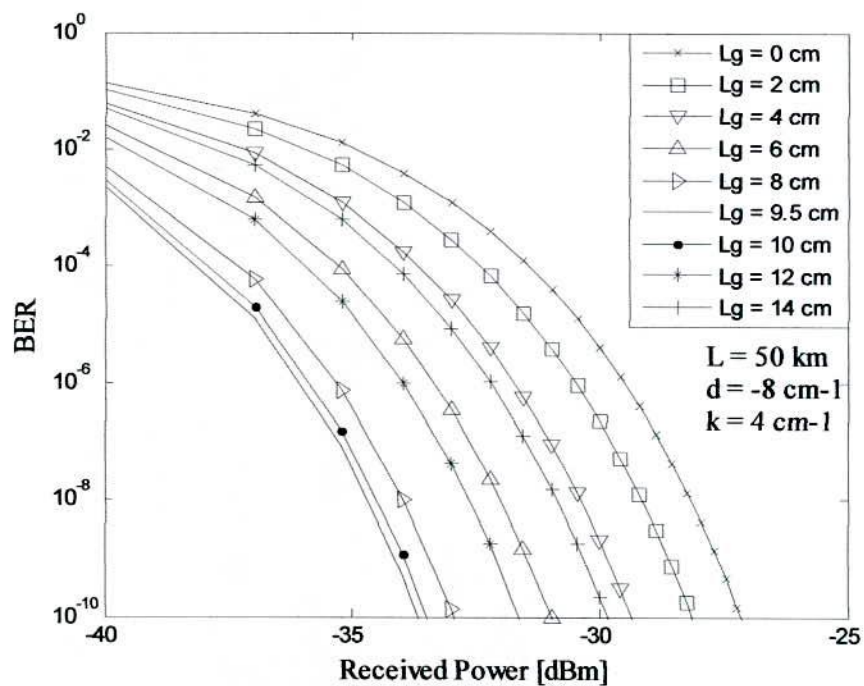
Fig. 4.8: Plot of BER versus received power as a function of fiber Bragg grating length for chip rate = 40Gchip/s, and fiber length = 50km.
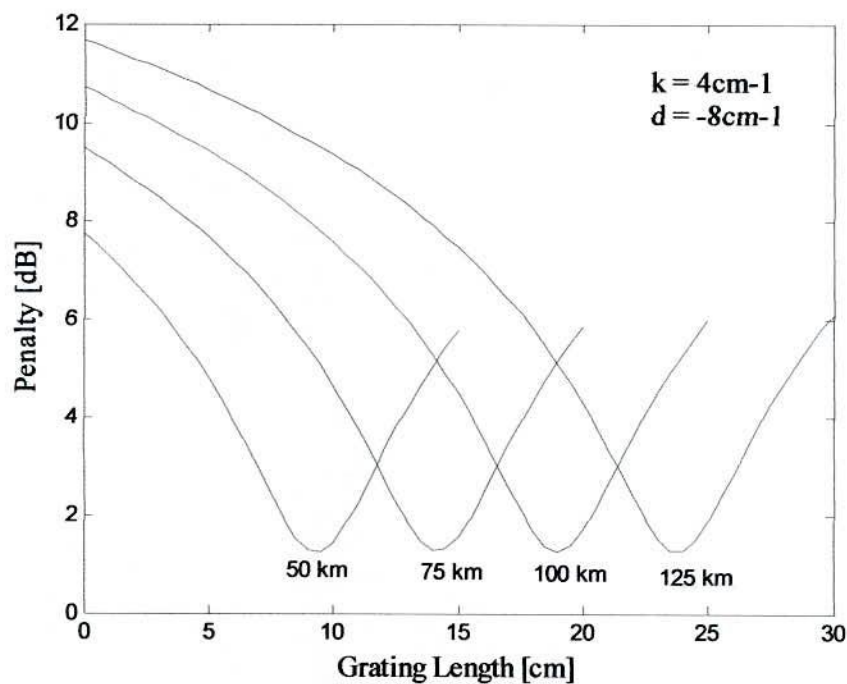

Fig. 4.9: Plot of power penalty versus fiber Bragg grating length for different fiber lengths when chip rate = 40Gchip/s, detuning $=-8cm^{-1}$, and coupling strength=$4cm^{-1}$.
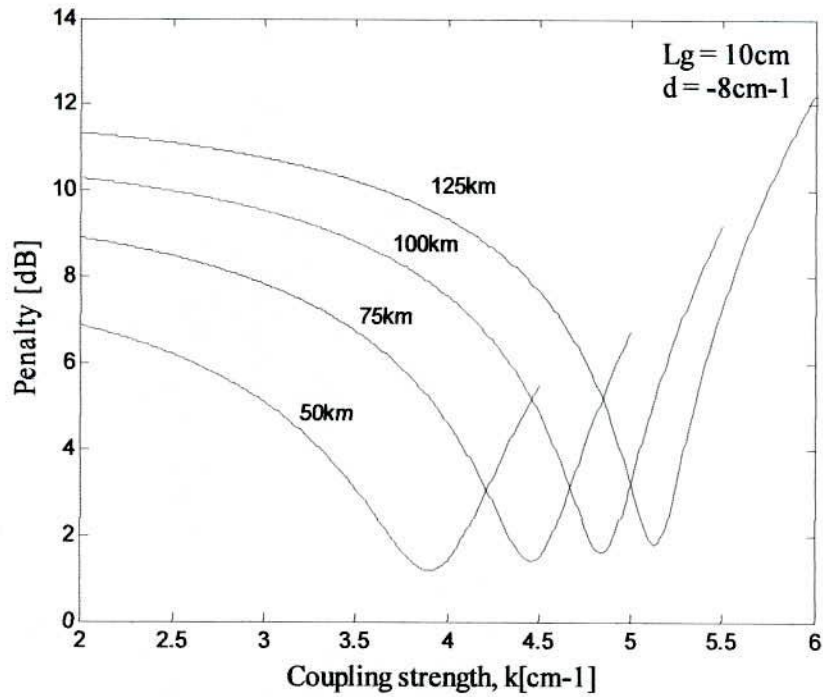
Fig. 4.10: Plot of power penalty versus coupling strength for different fiber lengths when chip rate = 40Gchip/s, detuning =-8cm^{-1}, and grating length = 10cm.
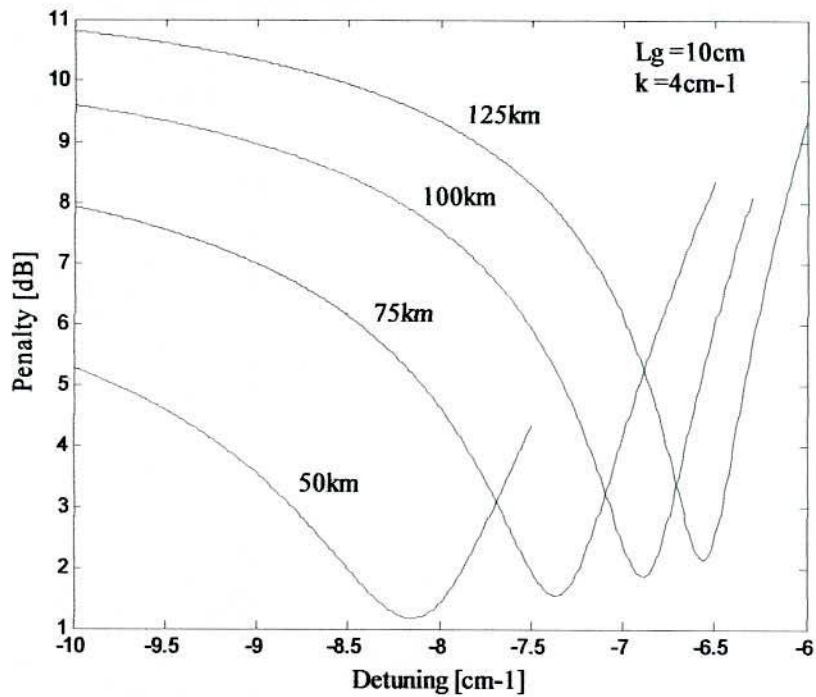
Fig. 4.11: Plot of power penalty versus detuning for different fiber lengths when chip rate = 40Gchip/s, coupling strength =-8cm^{-1}, and grating length = 10cm.
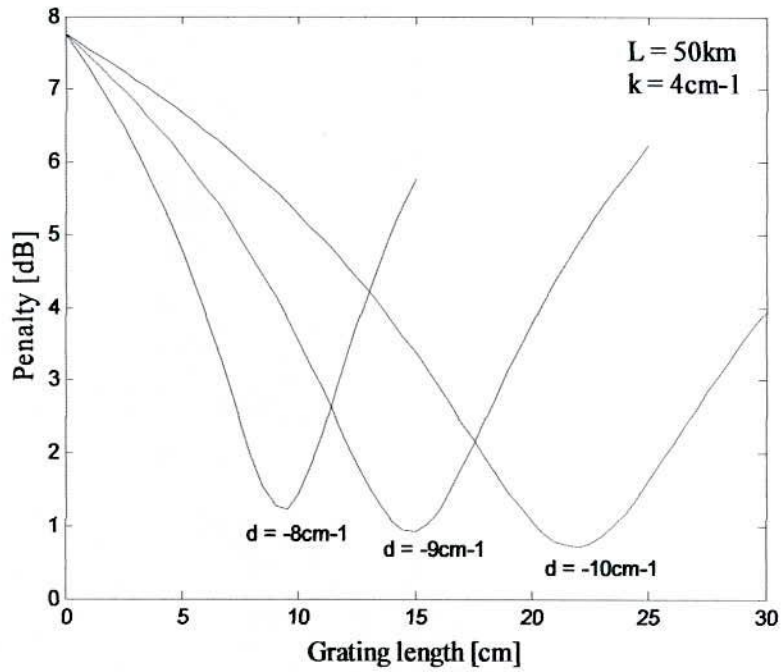
Fig. 4.12: Plot of power penalty versus fiber Bragg grating length for different detuning when chip rate = 40Gchip/s, fiber length = 50km, and coupling strength=4cm^{-1}.

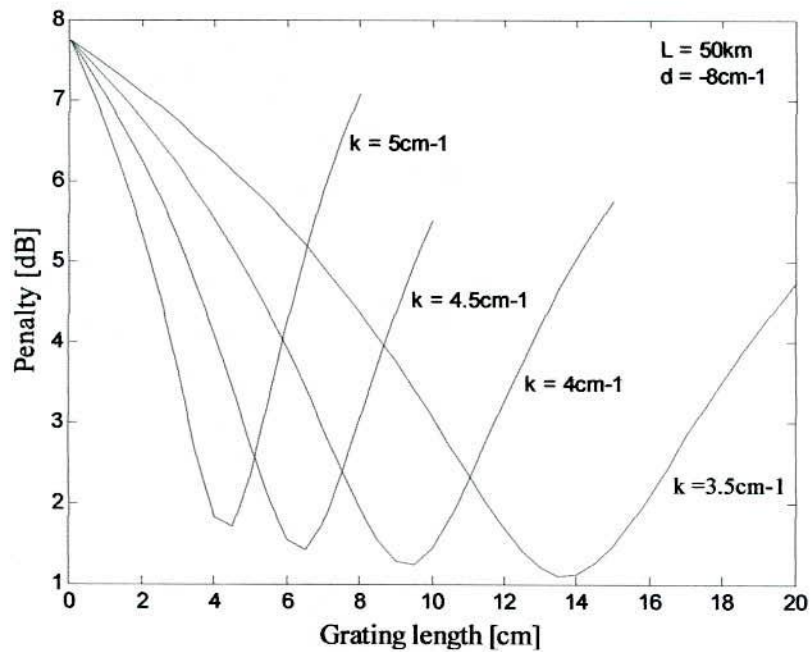Fig. 4.13: Plot of power penalty versus fiber Bragg grating length for different coupling strength when chip rate = 40Gchip/s, fiber length = 50km, and detuning=-8cm^{-1}.
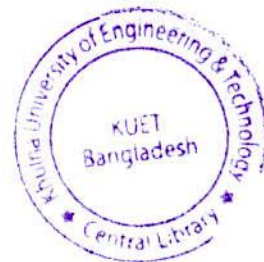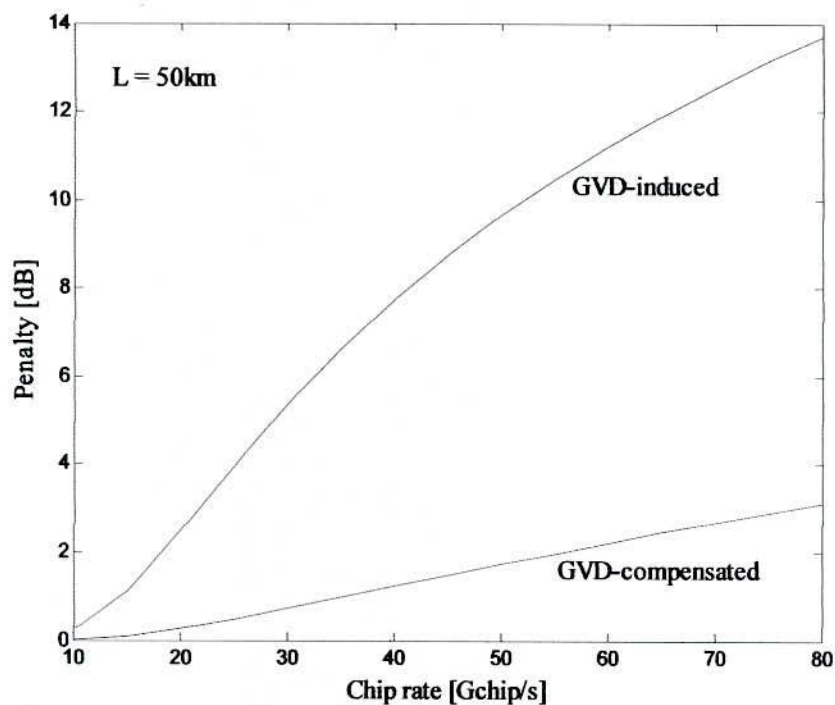
Fig. 4.14: Plot of power penalty versus chip rate in presence of only GVD, and FBG-based compensator at fiber length=50km.
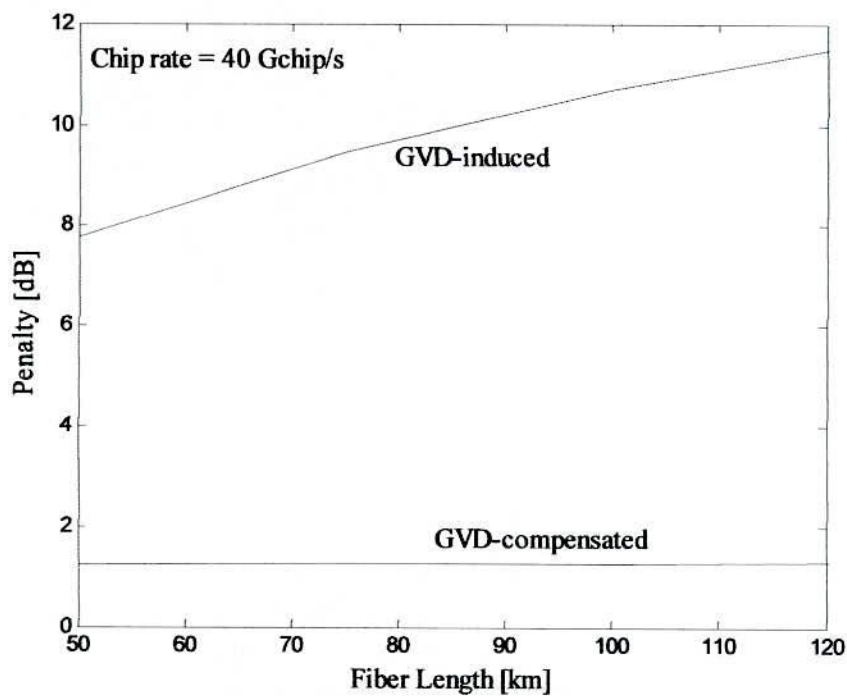

Fig. 4.15: Plot of power penalty versus fiber length in presence of only GVD, and FBG-based compensator at chip rate = 40Gchip/s.

Figure 4.15 depicts the plot of power penalty versus fiber length in presence of GVD and FBG-based GVD compensator at chip rate = 40Gchip/s. It is found that the power penalty increases linearly with increasing fiber length due to the effect of dispersion. Using FBG-based GVD compensator, the GVD-induced penalty can be compensated significantly but, can not be compensated totally. There are threshold penalty that occurs due to the effect of third order dispersion in the grating. The threshold penalty is found to be almost constant for different fiber lengths. Because, third-order grating dispersion is independent of grating length. The GVD-induced penalty is compensated about 90% using FBG-based compensator for the fiber length of 100km.

4.4 Performance Analysis in Presence of PMD

In conventional optical fiber communication system influence of PMD becomes prominent when bit rate is higher than 20Gb/s. Since a bit is converted into several chips with short duration in OCDMA system, impact of PMD will be severe in OCDMA. To understand the BER performance of the proposed OCDMA system in presence of PMD, the mathematical formulation presented in chapter 3 are used. In our calculation, Gaussian shaped OOC's are used as user address sequence. The parameters of the single mode fiber used for numerical computations are: PMD co-efficient $D_{PMD} = 0.5\,ps/\sqrt{km}$ at wavelength λ =1550 nm and fiber attenuation = 0.2dB/km. Also, assuming that the GVD-induced effect is compensated.

Figure 4.16 depicts the plot of BER versus number of simultaneous users for constant transmitted signal power. The results are evaluated for Gaussian-shaped chip with different values of fiber length L when chip rate = 80 Gchip/s. It is found that the BER performance of the proposed system is highly dependent on the number of simultaneous users as well as fiber length. The BER performance degrades with number of users due to the effect of MAI for all values of L. It is also found that for a particular number of users, the BER performance is aggravated with increasing fiber length due to the effect of PMD. This is because the amount of birefringence increases with increasing fiber length.
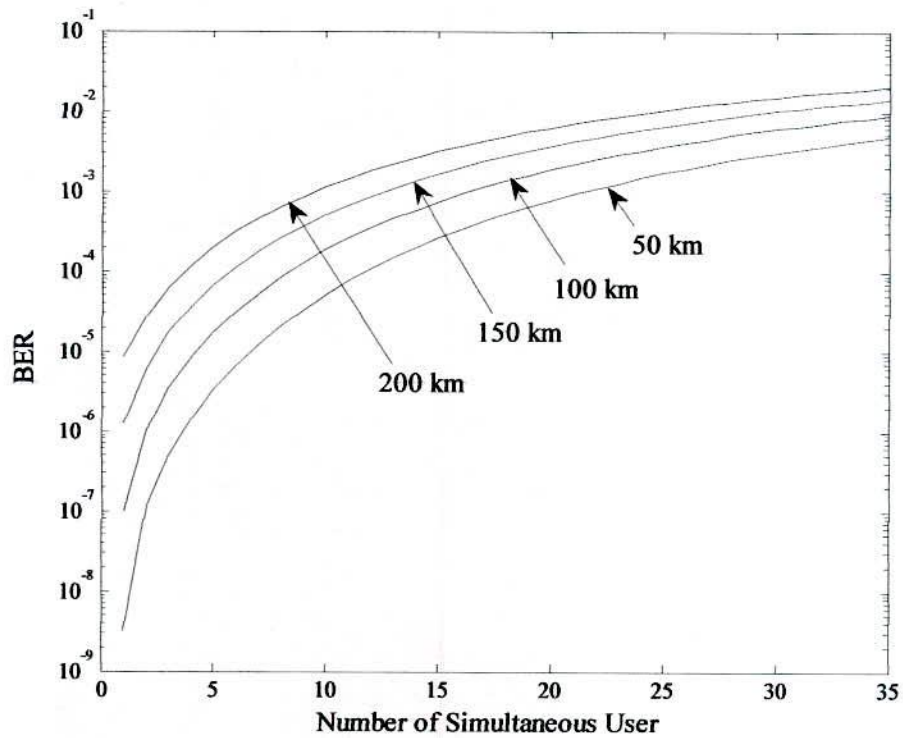
Fig. 4.16: Plot of BER versus number of simultaneous users with variable fiber length and constant chip rate = 80 Gchip/s.
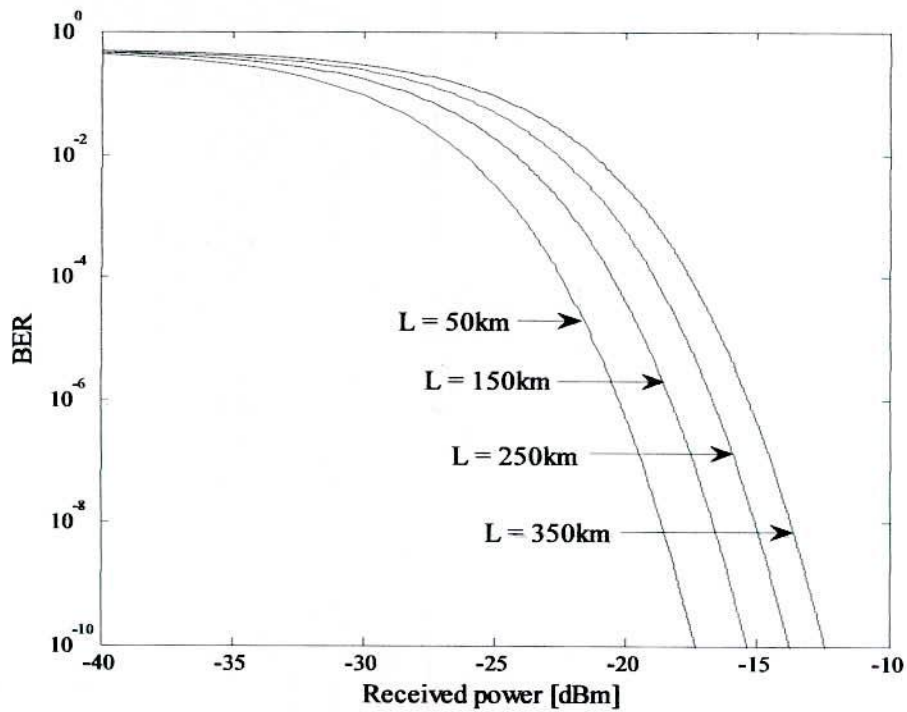
Fig. 4.17: Plot of BER versus received power for different fiber lengths when chip rate = 80 Gchip/s, and number of simultaneous user 10.
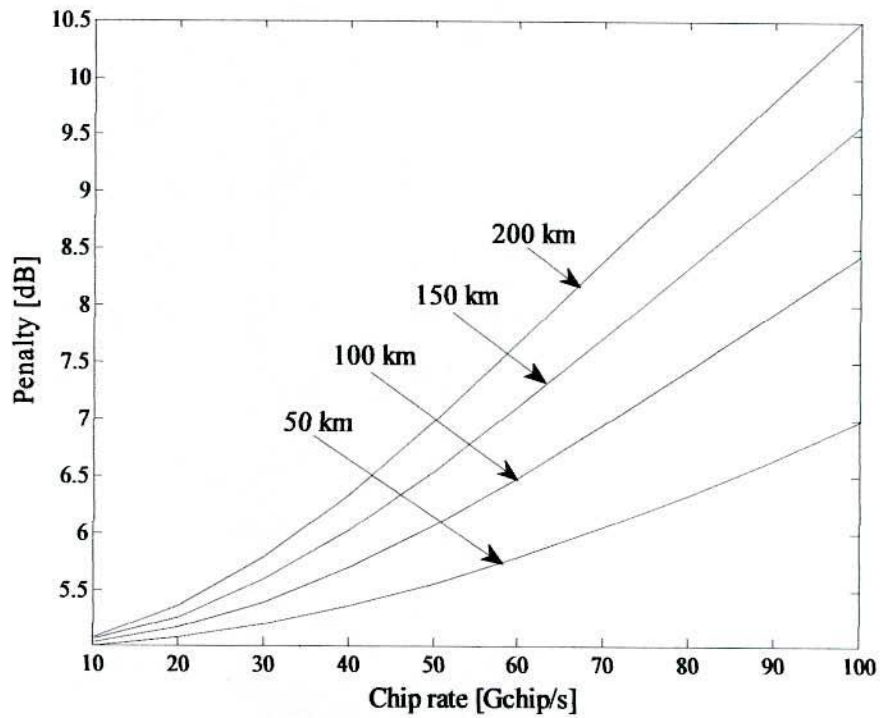
Fig. 4.18: Plot of power penalty versus chip rate for different fiber lengths when number of simultaneous users = 10.
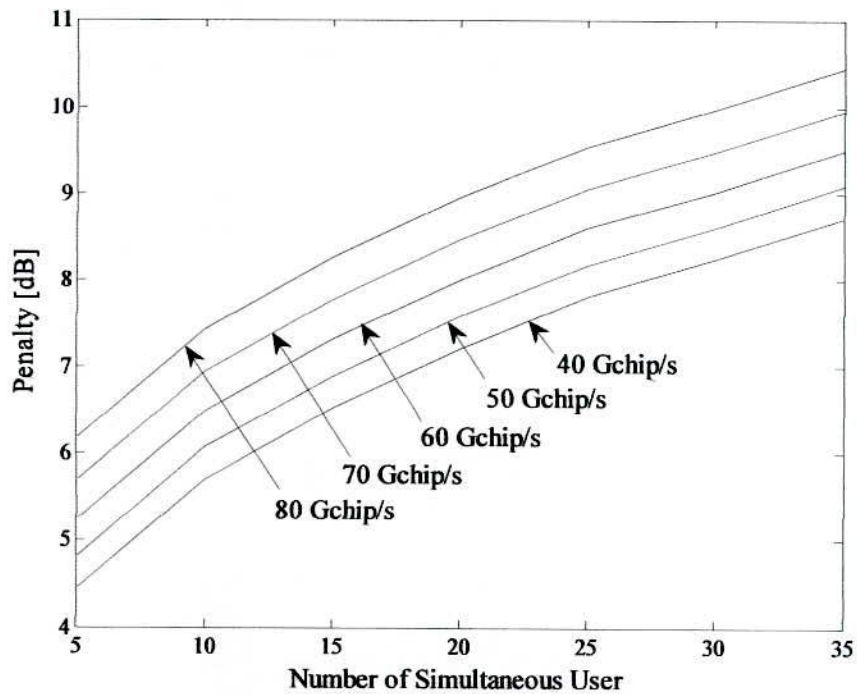
Fig. 4.19: Plot of power penalty versus number of simultaneous users with different chip rates when fiber length = 100km.

The BER performance is further plotted in Fig. 4.17 with respect to received power for different fiber lengths when chip rate = 80 Gchip/s, and number of simultaneous users 10. It is found that the amount of received signal power increases with increasing fiber length in order to maintain a constant BER of 10^{-9}, because the SNR goes below the base receiver sensitivity due to the effect of PMD.

The power penalty suffered by the system is determined at BER of 10^{-9} and plotted in Fig. 4.18 with respect to the chip rate for different fiber lengths. The results are determined for the simultaneous users 10. It is found that the power penalty increases with increasing chip rate due to the effect of PMD. It can be depicted that, with increasing chip rate, the chip duration becomes very short, consequently, the possibility of interchip interference increases between the adjacent chips due to the differential group delay resulted from PMD. The PMD-induced penalty is evaluated to be 3.28dB when chip rate increases from 10Gchip/s to 80Gchip/s for the fiber length of 150km. It is also found in Fig. 4.18 that the system suffers more penalties with increasing fiber length. The PMD-induced penalty increases from 6.345dB to 9.117dB with increasing fiber length from 50km to 200km for a constant chip rate of 80Gchip/s.

Figure 4.19 shows the plot of power penalty verses number of simultaneous users with variable chip rates. The results are determined for the fiber length=100km. It is found that the propose system suffers more penalty with increasing number of users due to the effect of MAI. It is also found that for a particular number of users, the system suffers more penalties with increasing the chip rate due to interchip interference caused by PMD-induced broadening of short duration chips.

4.5 Performance Evaluation in Presence of PMD Compensation

It is presumed that the BER performance of the proposed OCDMA can be improved by the PMD compensation using a suitable compensation technique. Using the mathematical formulations presented in chapter 3, the BER performance of the proposed system is further determined in presence of frequency advanced higher-order PMD compensation technique.

The power penalty suffered by the system is determined at BER of 10^{-9} as a function of chip rate. Figure 4.20 shows a comparison among the power penalties evaluated taking into account of PMD and different order of PMD compensation at chip rate of 80Gchip/s

and fiber length = 100km. The analysis is carried out for the PMD co-efficient $D_{PMD} = 0.5\,ps/\sqrt{km}$ and fiber attenuation = 0.2dB/km. It is found that the PMD-induced penalty is almost negligible below 20Gchip/s and increases sharply with increasing chip rate. This is because differential group delay between two principle states of polarization increases with increasing chip rate. The PMD-induced penalties are found to be compensated 1.59dB, 2.13dB, and 2.25dB, using the first-, second-, and third-order PMD compensations, respectively. It is also found in Fig. 4.20 that there is a constant penalty (~5dB) at lower chip rate that can not be compensated, because this penalty is due to MAI noise for the simultaneous users of 10.
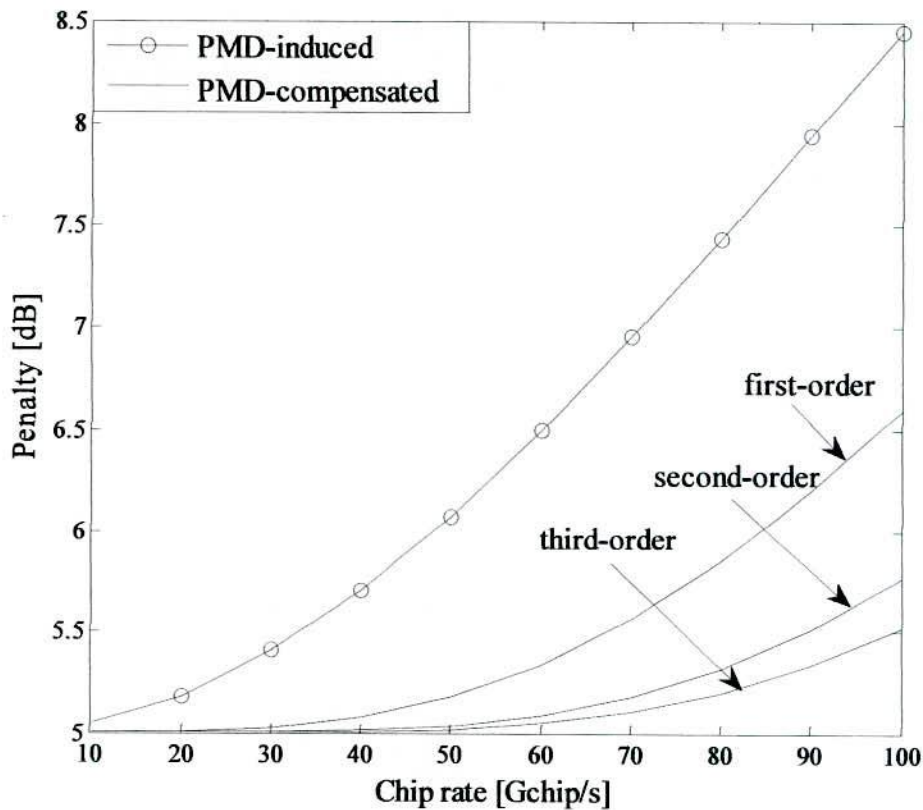
Fig. 4.20: Plot of power penalty versus chip rate at fiber length = 100km, and number of simultaneous users 10 in presence of PMD and PMD compensation.
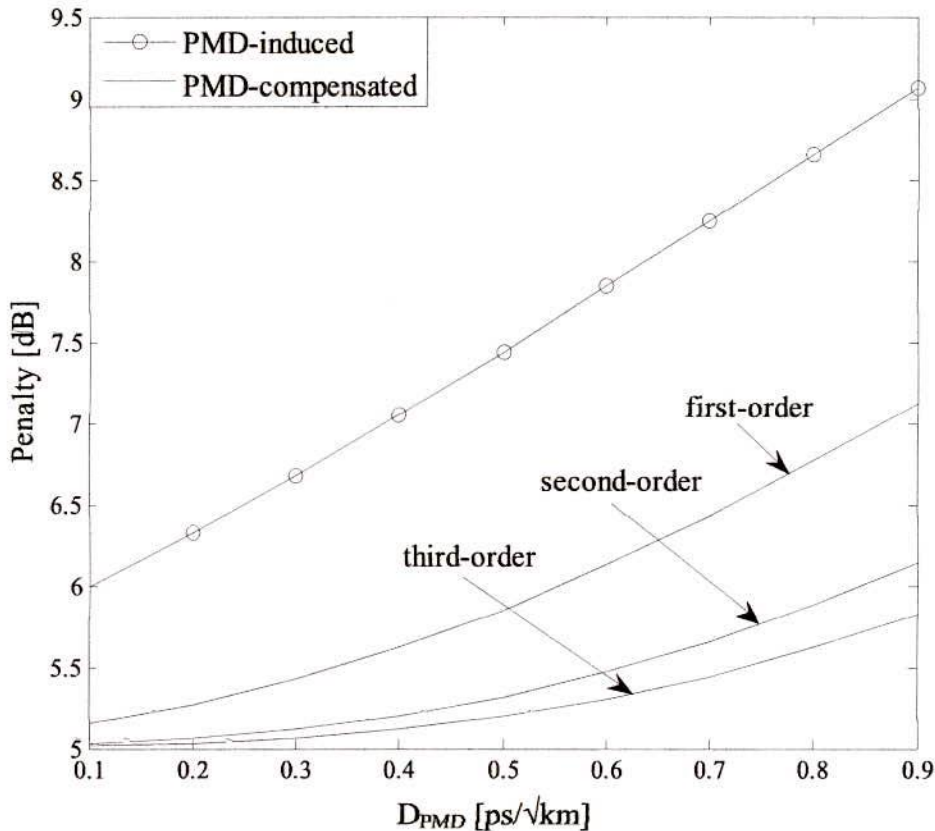
Fig. 4.21: Plot of power penalty versus PMD-coefficients at fiber length=100km, chip rate = 80Gchip/s, and number of simultaneous users 10 in presence of PMD and PMD compensation.

To understand the performance of PMD compensation in terms of PMD co-efficient the system BER performance is further evaluated for 100km fiber length, 80Gchip/s and number of users 10. The results are shown in Fig. 4.21 where the compensation performance found to improve with increasing PMD co-efficient. The results indicate that, using the first-, second-, and third-order PMD compensations, it is possible to compensate PMD-induced penalties approximately 1.94dB, 2.92dB, and 3.24dB, respectively, for the PMD-coefficient 0.9 ps/√km. The results presented in Figs. 4.20 and 4.21 indicate that using the frequency advanced higher order PMD vectors it is not possible to have full compensation. The results also indicate that third-order PMD compensation gives better results than the first-, and second-order compensations.

CHAPTER 5

Conclusion and Future Scope

5.1 Conclusion

We have analytically studied the impact of GVD on the performance of DS-OCDMA of a SMF operating at 1550nm. The analysis is carried out by Gaussian shaped OOCs. APD is used in the optical correlator receiver for optoelectronic conversion. The effect of receiver, optical amplifier, and MAI noises are considered to evaluate the BER performance. The power penalty suffered by the system at BER of 10^{-9} is determined as a function of fiber length, number of simultaneous user, and chip rate. The results obtained in the present study demonstrate that the system BER performance degrades severely due to GVD at longer fiber length. The typical value of power penalty changes from 7.54dB to 15.32dB for increasing the fiber length from 100km to 400km when chip rate is 10Gchip/s. It is also found that the BER performance of the proposed system degrades due to GVD with increasing chip rate. The system power penalty increases 7.16dB when chip rate is increased from 10Gchip/s to 25Gchip/s at fiber length=200km and number of simultaneous user=10. The power penalty is also found to increase from 6.04dB to 9.05dB when number of simultaneous user increases from 5 to 20 for the fiber length of 100km, and chip rate of 10Gchip/s.

We have further theoretically studied the chipshape-dependent performance of the proposed DS-OCDMA in presence of GVD. The analysis is carried out by OOCs with super-Gaussian-shaped and Hyperbolic-Secant-shaped chips using the same receiver as discussed above. The power penalty suffered by the system at BER of 10^{-9} is determined as a function of fiber length, number of simultaneous user, and chip shape. The results show that the proposed system suffers minimum power penalty for the Hyperbolic-Secant-shaped chip with respect to the super-Gaussian-shaped chip. The power penalty reduced by 0.63dB and 1.63dB for fiber length of 100km and 400km , respectively, when Hyperbolic-Secant-shaped chip is used and number of simultaneous users = 10.

We have also theoretically studied the improvement of BER performance of DS-OCDMA using FBG-based GVD compensator. The analysis is carried out by OOCs with Gaussian-shaped chip considering number of user = 1. The receiver and optical amplifier noises are

considered to evaluate the BER performance. The power penalty suffered by the proposed system at BER of 10^{-9} is determined as a function of compensator parameters, fiber length, and chip rate. The results show that there is an optimum grating length, detuning, coupling strength at which the proposed system suffers minimum power penalty for constant fiber length. It is found that about 90% of GVD-induced penalty can be compensated using FBG-based compensator when chip rate = 40Gchip/s, and fiber length = 100km.

Further, the BER performance of the proposed DS-OCDMA system is evaluated in presence of PMD. The results obtained in the present study demonstrate that the system BER performance degrades severely due to PMD at higher chip rate. The typical value of power penalty changes from 5.046dB to 7.44dB for increasing the chip rate from 10Gchip/s to 80Gchip/s when fiber length is 100km and number of user=10. It is also found that the BER performance of the proposed system degrades due to PMD with increasing transmitting fiber length. The system suffers power penalty from 6.054dB to 8.399dB when fiber length is increased from 50km to 200km at chip rate of 70Gchip/s and number of user=10. The power penalty is also found to increase from 5.244dB to 8.594dB when number of simultaneous users increase from 5 to 25 for the fiber length of 100km, and chip rate of 60Gchip/s. Since the performance of OCDMA severely degrades in presence of PMD, it is very much important to investigate the system performance in presence of PMD compensation. In order to do so frequency advanced higher-order PMD compensation technique is applied. It is found that the BER performance of the proposed system is improved significantly using PMD compensation. The PMD-induced penalty is reduced about 65%, 87%, and 92% using first-, second-, and third-order PMD compensations, respectively, at fiber length of 100km, and chip rate 80Gchip/s.

Finally it is concluded that significant improvement of the proposed OCDMA performance is possible by compensating GVD- and PMD-induced power penalties using FBG-based GVD compensator and frequency advanced higher-order PMD vector compensation techniques. Although theses compensation techniques give better results, full compensation is not possible using these techniques.

5.2 Future Scope

The present study is carried out on DS-OCDMA system considering the effects of GVD and PMD in fiber optic waveguide, and also the impact of GVD and PMD compensation are analyzed with different system parameters. OOC's are employed as address sequence. The future work can be extended employing gold and m-sequence user address. Sequence inversion keyed receiver can also be used in future analysis on account of other PMD and GVD compensators.

The DS-OCDMA system performance can be evaluated further considering various non-linear effects and their compensation techniques. The same analysis may be performed for FH-OCDMA and M-ary OCDMA system with in-line cascaded optical amplifiers.

References

[1] A J. Ratnam, "Optical CDMA in broadband communication: Scope and applications," *J. Opt. Commun.*, vol. 23, no. 1, pp. 11–21, Jan. 2002.

[2] G. Eisenstein, R. S. Tucker, and S. K. Korotky, "Optical time-division multiplexing for very high bit-rate transmission," *J. Lightw. Technol.*, vol. 6, no. 11, pp.1737–1749, 1988.

[3] M. S. Borella, et al., "Optical components for WDM lightwave networks," In proceedings of the IEEE, 1997.

[4] K. Iwatsuki, J. I. Kani, and H. Suzuki, "Access and metro metworks based on WDM technologies," *J. Lightw. Technol.*, vol. 22, no. 11, pp. 2623-2630, 2004.

[5] H. Kobrinski and K. W. Cheung, "Wavelength-tunable optical filters: applications and technologies," *IEEE Comm. Mag.*, vol. 32, no. 12, pp. 50–54, 1994.

[6] T. P. Lee and C. E. Zah, "Wavelength-tunable and single-frequency lasers for photonic communications networks," *IEEE Comm. Mag.*, vol. 27, no. 10, pp. 42–52, 1989.

[7] C. A. Brackett, "Dense wavelength division multiplexing networks: principle and applications," *IEEE J. on Selected Areas in Comm.*, vol. 8, no. 8, pp. 948–964, 1990.

[8] S. J. Kim, T. Y. Kim, and C. S. Park, "10-Gb/s temporally coded optical CDMA system using bipolar modulation/balanced detection," *IEEE Phot. Tech. Lett.*, vol. 17, no. 2, pp. 510-512, 2005.

[9] H. M. H. Shalaby, "Complexities, Error Probabilities, and Capacities of Optical OOK CDMA Communication Systems," *IEEE Trans. commun.*, vol. 50, no. 12, pp. 2009-2017, 2002.

[10] H. M. H. Shalaby, "Performance analysis of optical synchronous CDMA communication systems with PPM signaling," *IEEE Trans. Commun.*,vol. 43, pp. 624-634, 1995.

[11] S. A. Aljunid, M. Ismail, and A. R. Ramli, "A new family of optical code sequences for spectral-amplitude coding optical CDMA systems," *IEEE Phot. Tech. Lett.*, vol. 16, no. 10, pp. 2383-2385, 2004.

[12] V. K. Jain, "Performance evaluation of optical code division multiple access networks," *J. Opt. Commu.*, vol. 21, no. 3, pp. 110–115, 2000.

[13] Kambiz Jamshidi, and Jawad A. Salehi, "Performance Analysis of Spectral-Phase-Encoded Optical CDMA System Using Two-Photon-Absorption Receiver Structure for Asynchronous and Slot-Level Synchronous Transmitters," *J. Lightw. Technol.*, vol. 25, no. 6, pp. 1634–1645, 2007.

[14] M. Wehuna et al., "Performance analysis on phase encoded OCDMA communication system," *J. Lightw. Technol.*, vol. 20, no. 5, pp. 798–805, 2002.

[15] Chao Zuo, "The Impact of Group Velocity on Frequency-Hopping Optical Code Division Multiple System," *J. Lightw. Technol.*, vol. 19, no. 10, pp. 1416-1419, 2001.

[16] S.P. Majumder, Afreen Azhari, and F.M. Abbou, "Impact of fiber chromatic dispersion on the BER performance of an optical CDMA IM/DD transmission system," *IEEE phot. Tech. lett.*, vol. 17, No. 6, pp. 1340-1342, 2005.

[17] Xiaoqiang An, and Kun Qiu, "Influence of Single-mode fiber dispersion and pulse linear chirp on direct detection optical CDMA systems," *J. Opt. Commu.*, vol. 27, No. 1, pp. 20-25, 2006.

[18] Abdul Gafur, Doru Constantinescu, and Md Dulal Haque, "Evaluate the effect of dispersion of fiber on the performance of OCDMA system and to find the limitations imposed by dispersion on the number of user and length of transmission," *Canadian J. on Signal Processing*, vol. 1, no.1, pp. 1-6, 2010.

[19] W. Huang, et al., "Coherent optical CDMA (OCDMA) systems used for high-capacity optical fiber networks-system description, OTDM comparison, and OCDMA/WDMA networking," *J. Lightw. Technol.*, vol. 18, no. 6, pp. 765–778, 2000.

[20] Hyuck M. Kwon, "Optical Orthogonal Code-Division Multiple- Access System-Part I: APD Noise and Thermal Noise," *IEEE Trans. commun.*, vol. 42, no. 7, pp. 2470-2478, 1994.

[21] Anand Srivastava, Subrat Kar, and V. K. Jain "Performance Evaluation of PIN+OA and Avalanche Photodiode Receivers in Optical CDMA Networks," *J. Opt. Commu.*, vol. 22, no. 2, pp. 67–73, 2001.

[22] J.A. Salehi, "Code Division Multiple-Access Techniques in Optical Fiber Networks -Part I Fundamental Principles," *IEEE Trans. Commun.*, vol. 37, no. 8, pp. 824-842, 1989.

[23] J.A. Salehi, and C. Brackett, "Code Division Multiple-Access Techniques in Optical Fiber Networks –Part II System Performance Analysis," *IEEE Trans. Commun.*, vol. 37, no. 8, pp. 834-842, 1989.

[24] M. Brandt-Pearce and B. Aazhang, "Multiuser Detection for Optical Code Division Multiple Access Systems," *IEEE Trans. on Commun.*, vol.42, no. (2-4), pp. 1801-1810, 1994.

[25] C. Goursaud, "Parallel Multiple Access Interference Cancellation in Optical DS-CDMA systems," *Annals of Telecommunications*. Vol. 59, no. (9-10), pp. 1212-1227, 2004.

[26] F.N. Hasoon, S.A. Aljunid, M.K. Abdullah, and S. Shaari, "Construction of a new code for spectral amplitude coding in optical code-division multiple-access systems," *Optical Engineering Journal*, vol. 46, no. 7, pp. 75004-75008, 2007.

[27] M. M. N. Hamarsheh, H. M. H. Shalaby, and M. K. Abdullah, "Design and Analysis of a Dynamic Code Division Multiple Acces Communication System," *J. Lightw. Technol.*, vol. 23, no. 12, pp. 3959 -3965, 2005.

[28] Hilal A. Fadhil, Syed A. Aljunid, and R. Badlishah Ahmed, "Performance of Random Diagonal Codes for Spectral Amplitude Coding Optical CDMA Systems," *World Academy of Science, Engineering and Technology*, vol. 47, pp. 147-150, 2008.

[29] Nobuhiko Kikuchi, and Shinya Sasaki, "Analytical Evaluation Technique of Self-Phase-Modulation Effect on the Performance of Cascaded Optical Amplifier Systems," *J. Lightw. Technol.*, vol. 13, No. 5, pp. 868-878, 1995.

[30] N. M. Litchinitser, B. J. Eggleton, and D. B. Patterson, "Fiber Bragg gratings for dispersion compensation in transmission: Theoretical model and design criteria for nearly ideal pulse recompression," *J. Lightw. Technol.*, vol. 15, no. 8, pp. 1303–1313, 1997.

[31] Natalia M. Litchinitser, Benjamin J. Eggleton, and Govind P. Agrawal, "Dispersion of Cascaded Fiber Gratings in WDM Lightwave Systems," *J. Lightw. Technol.*, vol. 16, no. 8, pp. 1523–1529, 1998.

[32] Lih-Gen Sheu, Kai-Ping Chuang, and Yinchieh Lai, "Fiber Bragg Grating Dispersion Compensator by Single-Period Overlap-Step-Scan Exposure," *IEEE Phot. Tech. Lett.*, vol. 15, no. 7, pp. 939-941, 2003.

[33] Kenneth O. Hill and Gerald Meltz, "Fiber Bragg Grating Technology Fundamentals and Overview," *J. Lightw. Technol.*, vol. 15, no. 8, pp. 1263–1276, 1997.

[34] S. Xue-ming et al., "Impact of polarization mode dispersion and nonlinear effect on 40 Gbit/s dense wavelength division multiplexing system," *Front. Electr. Electron. Eng. China*, vol. 3, pp. 361–366, 2006.

[35] M. S. Islam and S. P. Majumder, "Effects of polarization mode dispersion on cross-phase modulation in a WDM optical transmission system," *International Journal for Light and Electron Optics*, vol. 122, no. 1, pp. 24-28, 2011.

[36] R. Khosravani, Y. Xie, L.S. Yan, A.E. Willner and C.R. Menyuk, "Bit pattern dependent polarization rotation in the first-order PMD-compensated WDM systems," *J. Opt. Commun.* Vol. 257, no. 1, pp. 191–196, 2006.

[37] Y. Zheng, B.J. Yang, and X.G. Zhang, "Analytical theory for pulse broadening induced by all-order polarization mode dispersion combined with frequency chirp and group-velocity dispersion," *Optical and Quantum Electronics*, vol. 35, pp. 725–734, 2003.

[38] Chongjin Xie, Linn F. Mollenauer, and Lothar Möller, "Pulse Distortion Induced by Polarization-Mode Dispersion and Polarization-Dependent Loss in Lightwave Transmission Systems," *IEEE phot. Tech. lett.*, vol. 15, no. 8, pp. 1073-1075, 2003.

[39] Magnus Karlsson and Henrik Sunnerud, "PMD impact on optical systems: Single- and multichannel effects," *J. Opt. Fiber Commun. Rep.*, vol. 1, no. 2, pp. 123–140, 2004.

[40] J. E. Baron, et al., "Multiple channel operation of an integrated acousto-optic tunable filter," *Eletronics Letters*, vol. 25, no. 6, pp. 375–376, 1989.

[41] M. Tachibana, R. I. Laming, P. R. Morkel, and D. N. Payne, "Erbium-doped fiber amplifier with flattened gain spectrum," *J. Lightw. Technol.*, vol. 3, pp. 118–120, 1991.

[42] A. Sneh and K. M. Johnson, "High-speed tunable liquid crystal optical filter for WDM systems," *in Proc. IEEE/LEOS Summer Topical Meetings on Optical Networks and Their Enabling Technologies*, 1994.

[43] A. R. Chraplyvy, et al., "Reduction of four-wave mixing crosstalk in WDM systems using unequally spaced channels," *IEEE Phot. Tech. Lett.*, vol. 6, no. 6, pp. 754–756, 1994.

[44] H. S. Hinton, "Photonic switching fabrics," *IEEE Comm. Mag.*, vol. 28, no. 4, pp. 71–89, 1990.

[45] H. G. Perros, "Connection-oriented networks: SONET/SDH, ATM, MPLS, and optical networks," John Wiley & Sons, 2005.

[46] B. Mukherjee, S. Yao, and S. Dixit, "Advances in photonic packet switching: an overview," *IEEE Comm. Mag.*, vol. 38, no. 2, pp. 84-94, 2000.

[47] G.P. Agrawal, "Fiber optic communication systems," John Wiley & Sons, New York, 3rd ed., 2002.

[48] Tancevski, L., Andonovic, I., "Wavelength hopping/time spreading code division multiple access systems," *IEE Electronics Lett.*, vol. 30, no. 17, pp. 1388-1390, 1994.

[49] Yegnanarayana, S., Bhushan, A., Jalali, B., "An inchoherent wavelength hopping/time spreading code-division mutliple access system," *Proceedings ECOC '99*, I-188, Nice, France, 1999.

[50] Yegnanarayana, S., Bhushan, A., Jalali, B., "Fast wavelength-hopping time-spreading encoding/decoding for optical CDMA," *IEEE Photonics Technology Letters*, vol. 12, no. 5, pp. 573-575, 2000.

[51] R. K. Chung, J. A. Salehi, and V. K. Wei, "Optical orthogonal codes: design, analysis, applications," *IEEE Transaction on Information Theory*, vol. 35, no. 3, pp. 595-604, 1989.

[52] A. A. Shaar, and P. A. Davies, "Prime sequences: Quasi-optimal sequences for or channel code division multiplexing," *IEE Electronics Letters*, vol. 19, no. 21, pp. 888-889, 1983.

[53] T. Ohtsuki, "Performance analysis of direct-detection optical CDMA systems with optical hard-limiter using equal-weight orthogonal signaling," *IEICE Trans. on Comm.*, vol. E82-B, no. 3, pp. 512-520, 1999.

[54] Gerd keiser, "Optical fiber communications", third edition, Mc- Graw-Hill Series in Electrical Engineering.

[55] John M. Senior, "Optical fiber communications," second edition, Principles and practice, 1999.

[56] J. P. Gordon and H. Kogelnik, "PMD fundamentals: Polarization mode dispersion in optical fibers," *Bell Laboratories, Lucent Technologies*, 2000.

[57] R.K. Boncek, A. McCurdy, and A. Sorby, "Polarization Mode Dispersion, Frequently Asked Questions," *ITU-T G.652 Characteristics of a single-mode optical fiber and cable*, 2003.

[58] R. Khosravani, I. T. Lima, E. Ibragimov, A. E. Willner and C. R. Menyuk, " Time and Frequency Domain Characteristics of Polarization-Mode Dispersion Emulators," *IEEE Photonics Technology Letters*, vol. 13, no. 2, pp.127-129, 2001.

[59] A. Sano, Y. Miyamoto, S. Kuwahara, and H. Tobo, "A 40 Gbps WDM Transmission with SPM/XPM Suppression Through Prechirping and Dispersion Management," *J. Lightw. Technol.*, vol. 18, no. 11, pp.1519–1527, 2000.

[60] G.P. Agrawal, "Nonlinear Fiber Optics," Third edition. Academic Press, An Imprint of Elsevier, 2001.

[61] H. Sunnerud, M. Karlsson, and P. A. Anderson, "Analytical theory for PMD-compensation," *IEEE Photon. Technol. Lett.*, vol. 12, pp. 50–52, 2000.

[62] Sangin Kim, "Analytical Calculation of Pulse Broadening in Optical Higher Order PMD Compensation," *J. Lightw. Technol.*, vol. 20, no. 7, pp. 1118-1123, 2002.

[63] M. Shtaif, A. Macozzi, and J. A. Nagel, "Mean-square magnitude of all-orders of polarization mode dispersion and the relation with the bandwidth of the principal states," *IEEE Photon. Technol. Lett.*, vol. 12, pp. 53–55, 2000.

List of Publications

International Journal Paper:

[1] **Md. Jahedul Islam**, and Md. Rafiqul Islam. "Impact of GVD and SPM on the Performance of DS-OCDMA," Academy Publisher Journal of Networks, ISSN: 1796-2056, vol. 06, no. 01, pp. 12-17, 2011.

[2] **Md. Jahedul Islam**, and Md. Rafiqul Islam, "Impact of Chip Shape on the Performance of DS-OCDMA in Presence of GVD and SPM," International Journal of Communication Networks and Information Security (IJCNIS), ISSN: 2076-0930, vol. 02, no. 03, pp. 178-183, 2010.

[3] **Md. Jahedul Islam**, and Md. Rafiqul Islam, "Impact of Optical Pulse Linear Chirp on the BER Performance of DS-OCDMA in Presence of Fiber Optic Dispersion," Pacific Journal of Science and Technology (PJST), ISSN: 1551-7624, vol. 11, no. 02, pp. 171-177, 2010.

[4] **Md. Jahedul Islam**, Kalyan Kumar Halder, and Md. Rafiqul Islam, "Effect of Optical Pulse Shape on the Performance of OCDMA in Presence of GVD and Pulse Linear Chirp," International Journal on Computer Science and Engineering (IJCSE), ISSN: 0975-3397, vol. 02, no. 04, pp. 1041-1046, 2010.

International Conference Paper:

[5] **Md. Jahedul Islam**, Mostafezur Rahman Talukdar, and Md. Rafiqul Islam. "Impact of Optical Fiber Dispersion and Self Phase Modulation on the Performance of DS-OCDMA". Proceedings of the 12th International Conference on Computer and Information Technology 2009, IUB, Dhaka, Bangladesh. [IEEE Xplore]

[6] **Md. Jahedul Islam**, Md. Rafiqul Islam, and S.P. Majumder, "Impact of Chipshape on the Performance of DS-OCDMA in Dispersive Fiber Medium," Proceedings of the 6th International Conference on Electrical and Computer Engineering 2010, BUET, Dhaka, Bangladesh. [IEEE Xplore]

[7] **Md. Jahedul Islam**, and Md. Rafiqul Islam, "Influence of Polarization Mode Dispersion on the BER Performance of DS-OCDMA," Proceedings of the 13th International Conference on Computer and Information Technology 2010, AUST, Dhaka, Bangladesh.[IEEE Xplore]